
**Rescaling Digital Fingerprints:
Techniques and Image Quality Effects**

MTR 95B0000061

June 1995

**D. J. Braunegg
R. D. Forkert
N. B. Nill**

Contract Sponsor: FBI
Contract No.: J-FBI-86-028(A)
Project No.: 04951510AA
Dept.: G034

Approved for public release; distribution unlimited.

© 1995 The MITRE Corporation. ALL RIGHTS RESERVED.

MITRE
Bedford, Massachusetts

Department Approval:

Joseph L. Howard
Department Head, G034

MITRE Project Approval:

William E. Zeiner
Project Leader, 04951510

ABSTRACT

This document describes techniques and image quality impacts of scanning/digitizing fingerprints at one resolution and rescaling (aka resampling) the digital images to another resolution. A number of rescaling techniques are investigated and 'good' as well as 'poor' techniques are identified. This work is in support of the Federal Bureau of Investigation - Integrated Automated Fingerprint Identification System (FBI - IAFIS), to aid and guide implementation of useful rescaling techniques that will retain required fingerprint image quality.

Keywords: Decimation, Digitizer, FBI, Fingerprints, IAFIS, Image Quality, Interpolation, Resampling, Rescaling, Scanner

TABLE OF CONTENTS

SECTION	PAGE
1 Introduction and Executive Summary	1
2 Aspects of Aliasing	5
2.1 General Explanation of Aliasing	5
2.2 Visual Effects of Aliasing	5
3 Rescaling Downward in Resolution Via Interpolation	11
3.1 Introduction	11
3.2 Rescaling Considerations	11
3.2.1 One-Dimensional Versus Two-Dimensional Analysis	12
3.3 Interpolation Functions	13
3.3.1 Decimation (Nearest Neighbor)	13
3.3.2 Bi-Linear Interpolation	14
3.3.3 Cubic Convolution	14
3.3.4 Two-Parameter Cubic Filters	15
3.3.5 Cubic B-Spline	15
3.3.6 Windowed Sinc Functions	15
3.3.6.1 Rectangular Window	16
3.3.6.2 Hann and Hamming Windows	16
3.3.6.3 Blackman Window	16
3.3.6.4 Kaiser Window	16
3.3.6.5 Lanczos Window	17
3.3.6.6 Gaussian Window	17
3.4 Evaluation of Interpolation Algorithms	18
3.4.1 Memory and Computational Requirements	21
3.4.2 Geometric Integrity	21
3.4.3 Qualitative Image Quality Assessment	21
3.4.4 Objective Image Quality Assessment of Fingerprints	31
3.4.5 Objective Image Quality Assessment via MTF	34
3.5 Implementation Details	35
3.6 Conclusions	36
4 Rescaling Downward in Resolution Via Decimation (Nearest Neighbor)	39
4.1 Uniform Decimation	39
4.2 Nonuniform Decimation	39
4.3 Decimation Effect on Geometric Accuracy	45
4.4 Implications	47

SECTION	PAGE
5 Rescaling Upward in Resolution	49
6 Identifying and Detecting Rescaling	53
6.1 Identifying a Good Rescaling Technique for Implementation	53
6.2 Detecting the Presence of an Unacceptable Rescaling Technique	53
List of References	55
Appendix A - Sampling Theory View of Aliasing	57
Appendix B - Modeling Decimation	59
Glossary	63

LIST OF FIGURES

FIGURE		PAGE
1	Ideal Frequency Spectrum of Pure Sine Wave	6
2	Sine Wave Images Rescaled to 500 ppi by Downward and Upward Rescaling Techniques	9
3	Test Image: Commercial Sine Wave Target and Inked Fingerprints	19
4	Original 600 ppi Composite Test Image	23
5	Composite Test Image Rescaled to 500 ppi (Decimation and Bi-Linear Interpolation)	23
6	Composite Test Image Rescaled to 500 ppi (Cubic Convolution, Two-Parameter Cubic Filter, Cubic B-Spline, and Rectangular Windowed Sinc)	25
7	Composite Test Image Rescaled to 500 ppi (Hann, Hamming, Blackman, and Kaiser Windowed Sinc)	27
8	Composite Test Image Rescaled to 500 ppi (Lanczos and Gaussian Windowed Sinc, and Two-Parameter Cubic Filter)	29
9	MTFs Associated with Interpolation Methods Not Exhibiting Visual Artifacts	34
10	MTFs Associated with Interpolation Methods Exhibiting Visual Artifacts	35
11	Pixel Locations of Sine Wave Image Decimated from 600 to 500 ppi	40
12	600 ppi Tribar Scan Rescaled to 500 ppi via Bi-Linear Interpolation and Decimation	43
13	Decimation Applied to a Pair of Ronchi Bars That Causes Maximum Separation	46

FIGURE		PAGE
14	Decimation Applied to a Pair of Ronchi Bars That Causes Minimum Separation	47
15	MTFs of 300 and 400 ppi Scanners Rescaled Upward to 500 ppi	50
A-1	Proper Nyquist Rate Sampling (Top Half) of a Signal Bandlimited to 10 cy/mm, and Improper Sampling Causing Aliasing (Bottom Half)	58
B-1	Spectrum of Three Pure Sinewaves (600 ppi)	60
B-2	Spectrum of Three Pure Sinewaves After 2:1 Decimation (300 ppi)	60
B-3	Spectrum of Three Pure Sinewaves After 3:2 Decimation (400 ppi)	61
B-4	Spectrum of Three Pure Sinewaves After 4:3 Decimation (450 ppi)	61
B-5	Spectrum of a 6 cy/mm Sinewave After 600 to 500 ppi Decimation	62

LIST OF TABLES

TABLE		PAGE
1	Assessment of Rescaling Algorithms	20
2	Objective and Subjective Assessments of Fingerprint Image Quality	33
3	Multi-Factor Analysis of Upward Rescaling of Sine Waves	51

SECTION 1

INTRODUCTION AND EXECUTIVE SUMMARY

This document reports on an investigation of various rescaling techniques that could commonly be applied to digital (scanned) fingerprints. Good, useful techniques as well as unsatisfactory techniques are discussed, with respect to their use in the Federal Bureau of Investigation's Integrated Automated Fingerprint Identification System (FBI-IAFIS). It is the intent of this document to supply information on rescaling which serves as a useful aid and guide to fingerprint system vendors, integrators, and users that are responsible for developing and implementing rescaling techniques for scanned fingerprints. Following the guidance in this document will help to assure the quality of digital fingerprints in IAFIS.

Fingerprint scanners to be used in IAFIS are required to produce images at specific pixels per inch (ppi) resolution levels: 250 ppi for text, 500 ppi for ten-print cards and live fingerprint scans, and 1000 ppi for latent fingerprints. However, it may often be more efficient, cost-effective, and convenient to employ scanners that have more than the required resolution. For example, it can be more efficient to scan an entire ten-print card at 500 ppi and then apply a rescaling algorithm to the top 3 x 8 inch text area of the card to achieve the 250 ppi required for that text area, rather than separately scanning the text area at 250 ppi. As another example, the true resolution of many of today's commercial-off-the-shelf (COTS) flatbed paper scanners is 600 ppi. Rather than paying the additional cost to modify these COTS scanners to scan cards at the required 500 ppi, it is more cost-effective to scan at the 'native mode' 600 ppi and then apply a rescaling algorithm to achieve 500 ppi. There are also many low cost COTS flatbed scanners operating at a true resolution of 300 or 400 ppi. A fingerprint system vendor or integrator may be tempted to utilize such a scanner and then rescale the output to achieve the required 500 ppi.

When rescaling the scanned image downward to achieve 500 ppi, the simplest method, commonly applied in COTS flatbed scanners, is to decimate the higher resolution image. Decimation simply removes specific rows and columns of pixels to reduce the size of the image. We previously demonstrated [Nill and Forkert, 1995] that 500 to 250 ppi decimation is an acceptable procedure for rescaling scanned text, in that retained image quality is more than adequate to decipher the text. On the other hand, the analysis detailed in Section 4 of this document demonstrates that 600 to 500 ppi decimation of digitized fingerprints creates visible image artifacts. These discontinuity artifacts can adversely affect the capability of fingerprint experts to perform fingerprint matching/identification, can adversely affect the feature detection capabilities of an Automated Fingerprint Identification System (AFIS), and can adversely interact with image compression. In addition, 600 to 500 ppi decimated images will periodically not meet the IAFIS Image Quality Specification's "geometric accuracy" requirement for scanners [FBI, 1994].

Given the image quality problems with 600 to 500 ppi decimation, a number of alternative rescaling techniques based on interpolation were investigated. As detailed in Section 3, these interpolation techniques prove to be superior to decimation in terms of retained image quality and lack of image artifacts. In addition, the geometric integrity of the original scan is substantially maintained.

An example is shown in Section 5 of the very apparent artifacts and low image quality produced when attempting to rescale upward, i.e., when scanning at a resolution less than 500 ppi and processing the image to obtain an effective 500 ppi image. This scanning approach is unacceptable for IAFIS scanners.

The analysis in this report supports the following conclusions regarding rescaling of digitized fingerprints:

(1) Rescaling 600 ppi scanned fingerprints to 500 ppi by decimation results in image artifacts and is an unsatisfactory technique. This type of decimation should be formally categorized as an unacceptable technique in the IAFIS IQS. Categorizing it as unacceptable requires a test procedure to detect it, and Section 6 discusses such detection methods. It is recommended that a quantitative detection method be implemented as part of the IAFIS IQS verification test procedures.

(2) Interpolation from 600 to 500 ppi is the preferred rescaling approach and this document describes a number of good interpolation techniques. These descriptions can be used as an aid and guide by those responsible for implementing scanner rescaling algorithms.

(3) Scanning at a true resolution which is less than 500 ppi and rescaling the image up to 500 ppi is unacceptable for IAFIS scanners, regardless of the rescaling technique used. Methods for detecting upward rescaling are discussed in Section 6.

Although the emphasis in this report is on exploring the various methods for producing 500 ppi resolution fingerprints, the same conclusions hold for the case of producing 1000 ppi resolution fingerprints. That is, if the fingerprint is scanned at a resolution higher than 1000 ppi then it should be rescaled to 1000 ppi via interpolation, and obtaining a 1000 ppi image from a scanner resolution of less than 1000 ppi would be unacceptable, no matter what method was used.

Another component of IAFIS consists of printers to produce hardcopy images of previously scanned/digitized fingerprints. To some degree, the analysis performed and conclusions drawn in this document with respect to rescaling scanner outputs also holds for rescaling printer outputs. However, there are several exceptions. In one case, rescaling upward for printing is a valid way of magnifying or enlarging the input digital image so that it can be more easily viewed, whereas upward rescaling of scanner outputs is unacceptable. In another case, printers which only print black/white dots and rely on 'dot dithering' to obtain grayscale, such as laserprinters or inkjet printers, may utilize complex algorithms tied to visual properties to obtain the dither pattern and gray scale values.

In these cases the best rescaling technique is effectively tied to the dither algorithm utilized, and no general statement can be made as to whether or not, e.g., decimation rescaling would give acceptable print image quality. On the other hand, the results and implications given in this document for rescaling scanner resolution downward would essentially hold true for downward rescaling of printers which do produce true gray scale pixels, such as digital photographic printers (e.g., dry silver printers).

SECTION 2

ASPECTS OF ALIASING

2.1 GENERAL EXPLANATION OF ALIASING

Aliasing is a term used to identify artifacts that come from undersampling a signal; these artifacts are undesirable because they either obscure real information or create false information. For example, aliasing could cause ridge-like false structures to appear in scanned fingerprints, or could cause real sweat pores to disappear. A discussion of aliasing from the perspective of signal processing sampling theory is given in Appendix A.

The degree of aliasing in three cases relevant to the IAFIS requirement for fingerprints to be digitized to 500 ppi are important to note, as follows:

- 1) A scanner that digitizes the fingerprint at a resolution less than 500 ppi (e.g., at 300 ppi) and then obtains an effective 500 ppi image by rescaling, will produce very significant aliasing artifacts.
- 2) A scanner that digitizes the fingerprint at a resolution greater than 500 ppi will produce visible artifacts if nonuniform decimation is used to reduce the higher resolution scan (e.g., at 600 ppi) to 500 ppi, but will not produce visible artifacts if an appropriate interpolation technique is used.
- 3) If the fingerprint is digitized at a true 500 ppi but the fingerprint itself has frequency content beyond the Nyquist frequency (resolution) of a 500 ppi scanner, then some aliasing will still occur. For example, the Nyquist frequency of a 500 ppi scanner is 9.8 cy/mm, but if the fingerprint has frequency content out to 12 cy/mm, then some aliasing will occur. Aliasing due to this cause is not normally visible, however, because of the normally low energy content of fingerprint spectra at frequencies above 9.8 cy/mm, and because the scanner's lens, which acts as a pre-sampling anti-aliasing filter (Nordbryhn, 1983), further suppresses the aliasing.

2.2 VISUAL EFFECTS OF ALIASING

The various rescaling techniques are described in the following sections, but it is instructive to first show the visual effects of aliasing due to image rescaling, in both the spatial domain and spatial frequency domain. It will be seen that some imaging problems are visible in the spatial domain, but others are more apparent and are quantifiable in the Fourier spatial frequency domain. For reference, Figure 1 illustrates an ideal case of a pure 5 cy/mm sine wave sampled at 500 ppi, where the Nyquist frequency equals 10 cy/mm. This ideal case produces just three energy spikes in the Fourier transform magnitude frequency domain. The intensity of the center spike is proportional to the average gray level of the sine wave, the locations of the two side spikes along the frequency axis (symmetrical around center spike) correspond to the spatial frequency of

the sine wave, and the intensity of a side spike is proportional to the peak-to-valley contrast of the sine wave.

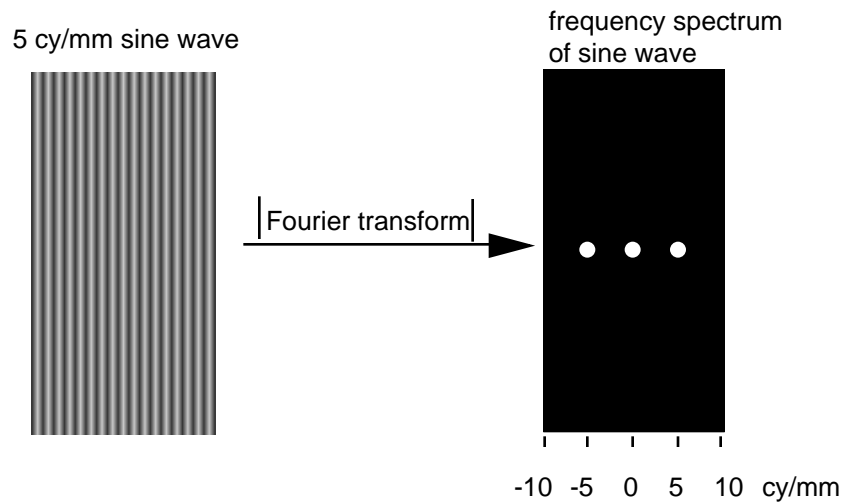


Figure 1. Ideal Frequency Spectrum of Pure Sine Wave

Figure 2 illustrates upward and downward rescaling to 500 ppi, via decimation and interpolation, of sine wave targets scanned on real scanners, and compares these to a non-rescaled scan originally obtained at 500 ppi. The left side in Figure 2 shows the images of 10, 8, 6, 5, and 4 cy/mm sine waves for each case and the adjacent right side shows the same sine wave images with the frequency spectrum for each sine pattern. Decimation, bi-linear interpolation, and the frequency spectra via the Fast Fourier Transform (FFT), were computed using a commercial image processing software package¹. Banding seen on a sine pattern shows up as secondary energy spikes in the Fourier domain, indicative of aliasing. The cause of the rays emanating vertically from the energy spikes was identified experimentally; these were found to be due to a small but steady increase in average gray level from top to bottom of each sine wave pattern on the target itself, combined with a small, but non-zero skew angle ($<1^\circ$) between the scanner detector array and axes of the sine target being scanned. These small gray scale "wedging" and skew effects are not visible in the spatial domain.

A description of each of the six cases presented in Figure 2 follows. Note that all of the figures containing images (Figures 2, 3-8, and 12) are available in their original softcopy form for more detailed assessment².

Rodh - This is the image from a Lenzar scanner operating at a true 500 ppi (sine scan supplied by the FBI); it typifies a good result on a real scanner, close to the ideal case illustrated in Figure 1. The sine waves are 'clean', in that no aliasing artifacts are visible.

¹ Media Cybernetics' MS-DOS program: *ImageProPlus (v2.0)* was used; this software computes the logarithm of the FFT spectrum magnitude for display purposes.

² Full resolution softcopy versions of Figures 2, 3-8, and 12 are available.

The predominant energy spikes in the frequency spectra occur at the single frequency corresponding to each sine wave's frequency, although some weak secondary spikes also do occur. These secondary spikes could be the result of weak sine wave harmonics in the target itself, due to the difficulty of manufacturing distortionless, 100% pure, continuous tone, sine wave targets on photographic paper.

Ricoh - This is an image from a Ricoh model IS-60 scanner operating at 600 ppi, which was then decimated to the 500 ppi image shown (500 ppi sine image supplied by FBI). Banding is very noticeable at 10, 6, and 5 cy/mm and the corresponding frequency spectra have several secondary energy spikes, all indicative of aliasing. The frequency spectra also have additional energy spikes near the top and bottom edges. These indicate another periodic pattern is overlaid on the basic sine wave pattern, but in a perpendicular direction. Measurements indicate that this overlaid pattern has a 7.9 cy/mm frequency, corresponding to 2.5 pixels or 2.5 scan lines per period. This anomaly may be caused by a periodic variability in the Ricoh's one-dimensional scanning operation, or may be the result of post-scan processing that used some variant of straightforward decimation.

Eik1 - Our in-house Eikonix model 1412 scanner was set up to scan at 600 ppi and the resulting image was scaled down to 500 ppi using simple decimation. Note that the banding in the sine waves and the occurrence of secondary energy spikes in the frequency spectra are nearly identical to the *Ricoh* image (except for the off-axis Ricoh spikes). The banding and secondary spikes, taken together, are the typical result obtained when 6:5 decimation is applied to a sine wave image.

Eik2 - The same 600 ppi scanned image used to generate *Eik1* was used to generate this 500 ppi image using bi-linear interpolation. Note that banding disappears in the sine patterns although some weak secondary energy spikes still occur in the frequency spectra of the 10 and 8 cy/mm sine patterns. This implies that some aliasing is still present, but not enough to be noticeable in the spatial domain. The sine patterns look very similar to the non-rescaled 500 ppi images in *Rodh*.

Eik3, Eik4 - The Eikonix was set up to scan at 300 ppi. *Eik3* and *Eik4* represent the scanned image scaled upward to 500 ppi via replication and bi-linear interpolation, respectively. The sine patterns in both images have very low contrast, banding is seen on *Eik3* at 6 and 5 cy/mm, and many secondary energy spikes occur in the frequency spectra, indicative of strong aliasing.

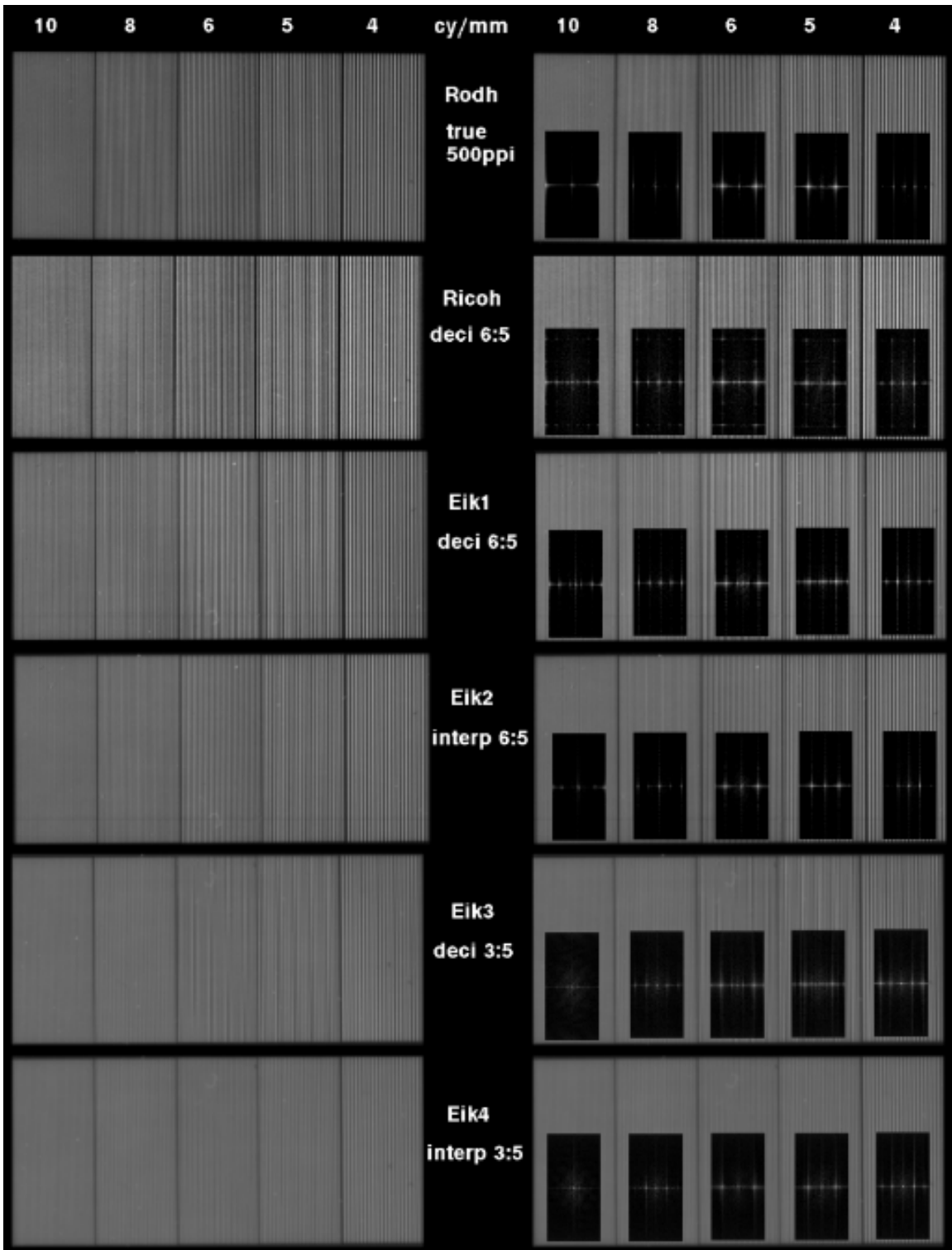


Figure 2. Sine Wave Images Rescaled to 500 ppi by Downward and Upward Rescaling Techniques

SECTION 3

RESCALING DOWNWARD IN RESOLUTION VIA INTERPOLATION

3.1 INTRODUCTION

It will be seen in Section 4 that rescaling downward in resolution via nonuniform decimation (e.g., 600 to 500 ppi) results in unsatisfactory image quality and periodic loss of geometric integrity. It will be seen in Section 5 that rescaling upward in resolution (e.g., 300 to 500 ppi), by any method, results in unacceptable image quality. This leaves rescaling downward in resolution via interpolation as the remaining practical possibility when rescaling is necessary. Fortunately, as will be seen in this section, downward interpolation rescaling is in fact an acceptable fingerprint image rescaling technique.

Several attributes of a rescaling algorithm need to be evaluated before selecting it. These relate to image quality, in terms of the appearance of image artifacts, the measurement of the MTF, and the application of other objective image quality measures. In addition, image integrity ("geometric accuracy") is important, and algorithm implementation also needs to be considered, i.e., computational complexity and memory requirements. It is noteworthy that the original image may be satisfactory in all of these areas while the down-sampled image may be deficient in one or all of these areas. The remainder of this section explores these attributes for the application of downward rescaling via interpolation, with the conclusion that a number of specific interpolation techniques are acceptable for use in the IAFIS fingerprint environment.

Typical parameter values for the interpolation functions were chosen for the evaluations, but an exhaustive optimization study was not performed. The intent was to present a variety of usable techniques and give some indication of usable and unusable parameter setting values. Although true optimization of each technique was beyond the scope and purpose of this study, a group of candidate 'good' techniques with useful starting parameter values can be ascertained from the information given in this section.

3.2 RESCALING CONSIDERATIONS

If the pixels in an image are thought of as points on a surface (where the pixel gray level value denotes height), then image rescaling can be thought of as reconstructing the continuous surface from those points, followed by resampling the surface at the new scale. The reconstruction process can be eliminated only when the input resolution is an integer multiple of the desired output resolution (e.g., 600 ppi input and 300 ppi desired output resolution), because the output pixels will then coincide exactly with the locations of the input pixels. This is the case for uniform decimation.

The reconstruction process is typically accomplished by applying an interpolation function to the original image. The subsequent resampling process is the same for any given interpolation function; the reconstructed image is sampled uniformly to obtain the

final image at the desired scale. Note that the choice of the interpolation function affects the appearance of the final, rescaled image, but the resampling process is completely determined by the input and output resolutions. Therefore, our discussion of rescaling will focus on the interpolation functions used in the reconstruction step.

3.2.1 One-Dimensional Versus Two-Dimensional Analysis

In the literature, most reconstruction algorithms are presented for one-dimensional (1-D) signals [Crochiere and Rabiner, 1983]. An image is (obviously) a two-dimensional (2-D) signal. The question then is, how should a given 1-D interpolation function be implemented in 2-D? One possibility is to implement a 2-D circularly-symmetric function based on the 1-D function. Distances along the 1-D function's abscissa axis would become Euclidean distances in the 2-D function. Certain 2-D circularly-symmetric functions (such as Gaussians) can be separated into 1-D functions, allowing first a 1-D pass over the rows of an image, then a 1-D pass over the columns (or vice versa). Such *separable* functions simplify the computational requirements of a 2-D interpolation function. Most functions, however, are not separable and, if they are to be used, the full 2-D functions must be implemented.

A second question concerning the 2-D implementation of an interpolation function is the original intent of the 1-D function. Many 1-D interpolation functions, especially those based on the sinc function

$$\begin{aligned} \text{sinc}(x) &= (\sin \pi x)/\pi x & x \neq 0 \\ \text{sinc}(x) &= 1 & x = 0 \end{aligned}$$

are designed such that, when the function is centered on an original input sample in a regularly-spaced set of samples, the function is zero-valued at all samples except the one at the center of the function, where the value of the function is unity. The interpolation function thus passes exactly the value of an input sample on which it is centered. If the function is not centered on an input sample, then its output is composed of contributions from several surrounding input samples. If a 2-D circularly-symmetric interpolation function is formed from such a 1-D function, then the 2-D function will be zero-valued at input samples directly horizontal and vertical from the sample at the function's center, but the function will be non-zero at other input samples. Thus, the 2-D interpolation function will *not* pass exactly the value of a sample on which it is centered.

Because of these two considerations, all of the interpolation functions mentioned in Section 3.3 are described as 1-D functions that are implemented in 2-D in terms of a pass over the columns followed by a pass over the rows (or, equivalently, rows followed by columns). Three of these functions have straightforward implementations directly in 2-D: Decimation, Nearest Neighbor, and Bi-Linear Interpolation [Wolberg, 1992, page 59].

3.3 INTERPOLATION FUNCTIONS

Twelve different interpolation functions, most with a range of parameter values, were applied to the case of rescaling a 600 ppi scanned image to 500 ppi. These functions are discussed in detail by Wolberg and the following discussion is derived from that work [Wolberg, 1992]. Most of the functions can be expressed as an interpolation kernel h to be convolved with the input image to obtain the output image. Because each of the interpolation kernels discussed below is symmetric about its central point, an equivalent method of determining an output pixel value is to center the kernel in the input image at the location of the output image, then sum the products of the input image samples and the corresponding kernel values. Recall that the 1-D interpolation function should first be passed over the columns of the input image to form an intermediate image, then passed over the rows of the intermediate image to form the final, rescaled image (or vice versa).

For each interpolation function, the width of the sampling neighborhood is always chosen to be odd so that the interpolation kernel is symmetric on each side of the central value. Note that for some algorithms, particularly bi-linear interpolation, application of an interpolation kernel may not be the most efficient implementation possible.

3.3.1 Decimation (Nearest Neighbor)

The simplest rescaling method is *decimation*. Although decimation is not an interpolation technique, it is included in this section for comparison purposes. The output image is obtained by using the ratio between the input and output resolutions to map input pixels to output pixels. For resampling from 600 ppi to 500 ppi, decimation drops every sixth row and every sixth column of pixels. For example, let $f_{600}(x, y)$ describe the pixel gray level values of a 600 ppi image and $f_{500}(x, y)$ be the values of a 500 ppi image, where pixels occur at integer values of x and y and where $(0, 0)$ denotes the upper left-hand corner pixel. To convert the 600 ppi image to 500 ppi by decimation, the value of each pixel at (x, y) in the 500 ppi image is

$$f_{500}(x, y) = f_{600}(\lfloor 6x/5 \rfloor, \lfloor 6y/5 \rfloor)$$

where $\lfloor x \rfloor$ denotes the floor of x , the largest integer not greater than x .

Decimation can also be implemented by first decimating all of the rows, then the resultant columns (or vice versa). Each row (or column) pixel value is determined by $f_{500}(x) = f_{600}(\lfloor 6x/5 \rfloor)$. The two methods of implementing decimation are equivalent; for the 600 ppi rescaled to 500 ppi case, both methods have the effect of dropping every sixth row and every sixth column of pixels.

In *nearest neighbor* rescaling, each output pixel is assigned the value of the nearest input pixel. For rescaling from 600 ppi to 500 ppi, the nearest neighbor algorithm has the effect of dropping every third row and column out of every set of six. This conversion can be expressed by the following equation, where again, $(0, 0)$ is the upper left image pixel:

$$f_{500}(x, y) = f_{600}(\lfloor 6(x+3)/5 \rfloor - 3, \lfloor 6(y+3)/5 \rfloor - 3)$$

Note that nearest neighbor rescaling is essentially the same as decimation, with the only difference being which pixel in each set of six is dropped.

The periodic dropping of pixels inherent in nonuniform 6:5 decimation causes discontinuities which result in unsatisfactory images. For example, when this algorithm is applied to a sine wave test target, the output image exhibits a banding effect at certain frequencies where the dropped input sample causes a 'bunching' of the sine wave ridges. Nonuniform decimation is explored in more detail in Section 4.

3.3.2 Bi-Linear Interpolation

Linear interpolation passes a straight line through each succeeding pair of pixels (in a row or column) and determines intermediate values from the value of this interpolating line at any given location. This line constitutes a first-degree interpolating polynomial. Pixel values in the rescaled image that fall between the original pixels are intermediate values along the line. When the straight-line approximation is applied in both the vertical and horizontal directions, the method is known as *bi-linear interpolation*. For image rescaling, linear interpolation can be applied first to the rows, then to the resulting columns, or the interpolation can be applied in both directions at once. Although perhaps not the most efficient implementation of the algorithm, linear interpolation can be expressed as a convolution of the input image with an interpolation kernel h :

$$\begin{aligned} h(x) &= 1 - |x| & 0 \leq |x| < 1 \\ h(x) &= 0 & 1 \leq |x| \end{aligned}$$

For the interpolation kernels presented herein, one unit of x is the pixel-to-pixel distance in a row or column. Pixels in the output (rescaled) image occur at integer values of x .

3.3.3 Cubic Convolution

Cubic convolution is a third-degree interpolation algorithm. It approximates a sinc interpolation function and is based on a general cubic spline. The kernel is composed of piecewise cubic polynomials, where the pieces are continuous and have continuous first derivatives. A set of constraints on the convolution kernel yield a family of solutions with one free parameter a . The resulting interpolation kernel h is

$$\begin{aligned} h_a(x) &= (a+2)|x|^3 - (a+3)|x|^2 + 1 & 0 \leq |x| < 1 \\ h_a(x) &= a|x|^3 - 5a|x|^2 + 8a|x| - 4a & 1 \leq |x| < 2 \\ h_a(x) &= 0 & 2 \leq |x| \end{aligned}$$

Bounding the parameter a to values between -3 and 0 makes h resemble the sinc function. If $a = -1$, the slope of h matches that of the sinc function at $x = 1$. This choice of a

results in some high-frequency enhancement. If $a = -0.75$, the second derivatives of the cubic polynomials in h are both 1, yielding a continuous second derivative at $x = 1$. [An interpolation function with a continuous second derivative can yield an output that is smoother than that of one with a discontinuous second derivative.] Finally, if $a = -0.5$, the Taylor series expansion of the interpolating function agrees in as many terms as possible with the original signal. Also note that, in the general case, cubic convolution can result in output values outside of the range of the input values.

3.3.4 Two-Parameter Cubic Filters

By using a different set of constraints on the cubic convolution kernel, a family of solutions with two free parameters can be derived. An interpolation function in this family of solutions is known as a *two-parameter cubic filter* and the parameterized interpolation kernel h for such a filter is

$$\begin{aligned} h_{b,c}(x) &= [(-9b - 6c - 12)|x|^3 + (12b + 6c - 18)|x|^2 + (-2b + 6)] / 6 & 0 \leq |x| < 1 \\ h_{b,c}(x) &= [(-b - 6c)|x|^3 + (6b + 30c)|x|^2 + (-12b - 48c)|x| + (8b + 24c)] / 6 & 1 \leq |x| < 2 \\ h_{b,c}(x) &= 0 & 2 \leq |x| \end{aligned}$$

One choice for the free parameters is $b = 0.33$ and $c = 0.33$, which has been shown to yield good image quality [Schreiber 1985]. This function with parameters $b = 1.5$ and $c = -0.25$ corresponds to a notch filter that suppresses the signal near the Nyquist frequency that is most responsible for aliasing.

3.3.5 Cubic B-Spline

Cubic B-spline interpolation is based on a piecewise cubic function that is continuous and has continuous first and second derivatives. The B-spline interpolation kernel is

$$\begin{aligned} h(x) &= [3|x|^3 - 6|x|^2 + 4] / 6 & 0 \leq |x| < 1 \\ h(x) &= [-|x|^3 + 6|x|^2 - 12|x| + 8] / 6 & 1 \leq |x| < 2 \\ h(x) &= 0 & 2 \leq |x| \end{aligned}$$

Note that because $h(0) \neq 1$, $h(1) \neq 0$, and $h(2) \neq 0$, h is an approximating function that passes near, but not through, the original pixel values. This typically has the effect of attenuating the original signal.

3.3.6 Windowed Sinc Functions

According to sampling theory, the ideal interpolation kernel is the sinc function. Unfortunately, this function has infinite extent and is therefore not a practical interpolation function for use in rescaling. The sinc function can be truncated by multiplying it with a window function, thus requiring only the finite number of input samples that fall within the extent of the window.

The kernel for this class of windowed sinc functions has the form

$$h(x) = \text{window}(x) \text{sinc}(x)$$

We consider several possibilities for the window function $\text{window}(x)$.

3.3.6.1 Rectangular Window

The simplest window function simply truncates the sinc function outside a certain range of values and maintains its value within that range. This *rectangular window* is

$$\begin{aligned} \text{Rect}_a(x) &= 1 & 0 \leq |x| < 0.5a \\ \text{Rect}_a(x) &= 0 & 0.5a \leq |x| \end{aligned}$$

The choice of the parameter a determines the width of the rectangular window. This rectangular window, which sharply truncates the sinc function with no smoothing, typically causes a grid effect in the rescaled image (see Figure 6) and can also cause ringing.

3.3.6.2 Hann and Hamming Windows

The *Hann* and *Hamming windows* both consist of a scaled and shifted cosine. The Hann and Hamming window functions are both defined over N samples and are described by

$$\begin{aligned} \text{Hann}(x) \text{ or } \text{Hamming}(x) &= \alpha + (1 - \alpha) \cos(2\pi x / (N - 1)) & |x| < (N - 1)/2 \\ \text{Hann}(x) \text{ or } \text{Hamming}(x) &= 0 & \text{otherwise} \end{aligned}$$

differing only in the choice of α , which is 0.5 for the Hann window and 0.54 for the Hamming window. Some slight ringing effects can arise from the Hamming window because it is discontinuous at its ends.

3.3.6.3 Blackman Window

The *Blackman window* is similar to the Hann and Hamming windows, but contains an additional cosine term to help reduce ripple in the Fourier spectrum of the function:

$$\begin{aligned} \text{Blackman}(x) &= 0.42 + 0.5 \cos(2\pi x / (N - 1)) + 0.08 \cos(4\pi x / (N - 1)) & |x| < (N - 1)/2 \\ \text{Blackman}(x) &= 0 & \text{otherwise} \end{aligned}$$

3.3.6.4 Kaiser Window

The *Kaiser window* is based on a zeroth-order modified Bessel function of the first kind (I_0), with one free parameter α :

$$\begin{aligned} \text{Kaiser}_\alpha(x) &= I_0(\beta)/I_0(\alpha) & |x| < (N-1)/2 \\ \text{Kaiser}_\alpha(x) &= 0 & \text{otherwise} \end{aligned}$$

where,

$$\beta = \alpha[1 - (2x/(N-1))^2]^{1/2}$$

If the Bessel function is not available in a mathematics package for implementation of the Kaiser window, it can be approximated using the rapidly converging series

$$I_0(n) = 1 + \sum_{k=1}^{\infty} \left[\frac{1}{k!} \left[\frac{n}{2} \right]^k \right]^2$$

If a series expansion of the Bessel function is implemented, careful examination of the extent of the series needed to obtain satisfactory results is required.

The sophistication of the Kaiser window function grows with the parameter α , varying from a rectangular window at $\alpha = 0$ to an approximation of the Hamming window at $\alpha = 5$.

3.3.6.5 Lanczos Window

The L-lobed *Lanczos window* is the central lobe of a scaled sinc function that extends over L lobes of a standard sinc function:

$$\begin{aligned} \text{Lanczos}_L(x) &= (\sin(\pi x/L))/(\pi x/L) & 0 \leq |x| < L \\ \text{Lanczos}_L(x) &= 0 & L \leq |x| \end{aligned}$$

3.3.6.6 Gaussian Window

The *Gaussian window* is simply a Gaussian function of standard deviation σ that is truncated outside a window of N samples. The Gaussian window is defined as

$$\text{Gauss}_\sigma(x) = e^{-x^2/2\sigma^2}$$

Note that the usual leading fraction of the Gaussian, $1/(\sigma\sqrt{2\pi})$, has been dropped so that the value of the window function is unity at $x = 0$.

The rate of fall-off of the function is determined by the choice of σ . Because the tails of the Gaussian diminish rapidly, the interpolation function can be truncated without causing excessive ringing in the output signal once the value of the Gaussian is small.

3.4 EVALUATION OF INTERPOLATION ALGORITHMS

The rescaling algorithms described in Section 3.3 were implemented in 'C' on a SUN SparcStation 2. A commercial sine wave target, together with three inked right index fingerprints of differing qualities were scanned at 600 ppi on an Eikonix model 1412 scanner as shown in Figure 3. Each algorithm was then individually applied to the 600 ppi image to rescale it to 500 ppi. The algorithms were evaluated in terms of memory and computational requirements and the rescaled images were evaluated both quantitatively and qualitatively. Specifically, the images were viewed on a CRT display to detect any visible image artifacts and the Fourier transforms of sine wave patterns at 10, 6, and 4 cy/mm were displayed to detect aliasing. Also, the MTFs of the sine wave target images were computed and an objective image quality measure (IQM) was applied to the fingerprint images.

The evaluations of the rescaling algorithms in terms of computational requirements, IQM, MTF, and visual artifacts are summarized in Table 1. Note that the IQM and MTF measurements (described in Sections 3.4.4 and 3.4.5, respectively) are based on an image obtained by a particular scanner and may be different with an image obtained from a different scanner.

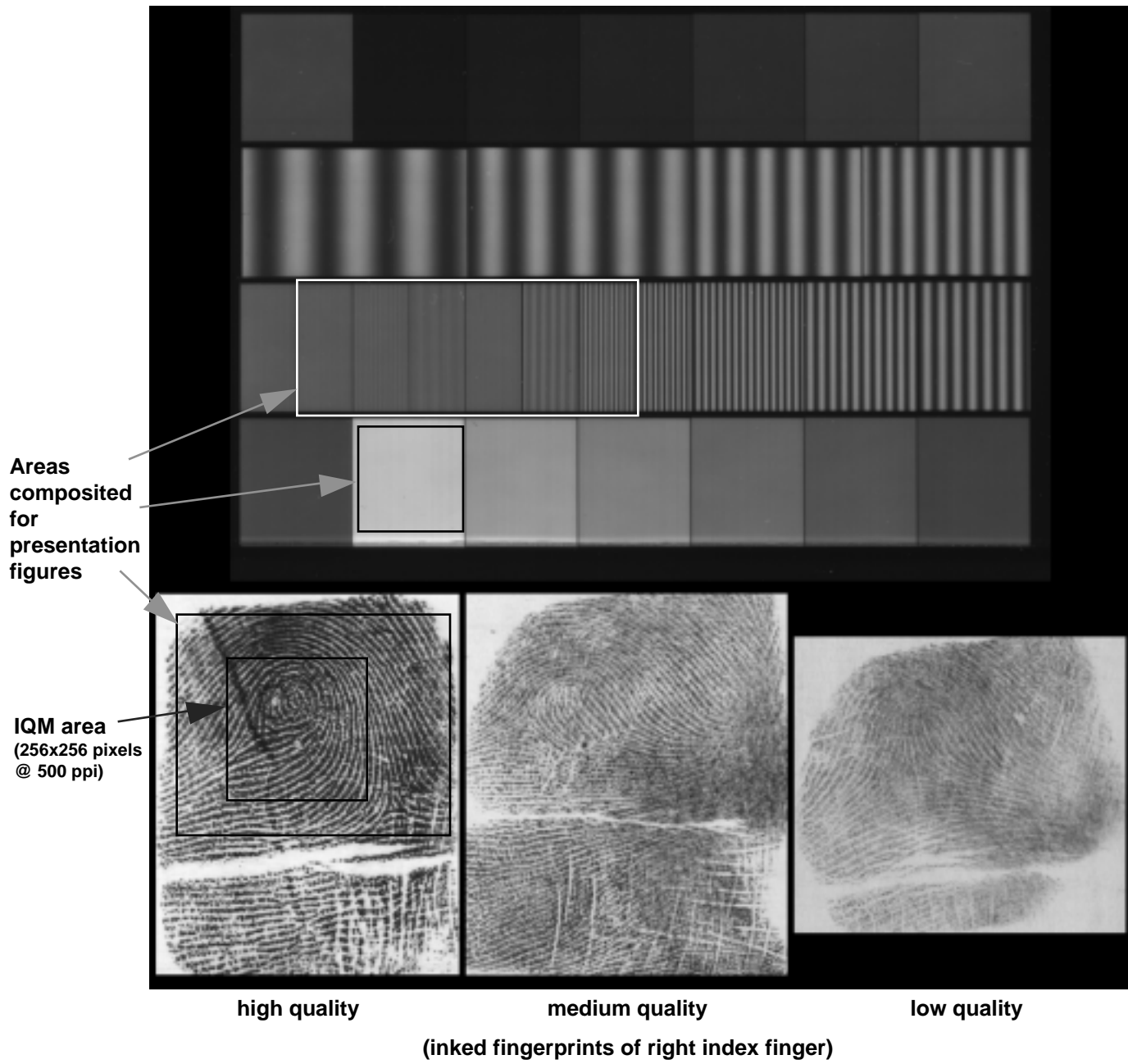


Figure 3. Test Image: Commercial Sine Wave Target and Inked Fingerprints

Table 1. Assessment of Rescaling Algorithms

Interpolation Technique	Computational requirements	IQM	MTF meets spec?	Visual artifacts
Decimation	Minimal	39.3	Yes	Banding
Bi-Linear Interpolation	Minimal	35.7	Yes	None
Cubic Convolution	square, cube, absolute value			
$a = -0.5$		38.1	Yes	None
$a = -0.75$		39.4	Yes	None
$a = -1.0$		40.7	Yes	None
Two-Parameter Cubic Filter	square, cube, absolute value			
$b = 0.33, c = 0.33$		36.0	Yes	None
$b = 1.5, c = -0.25$		29.9	No – too low	None
Cubic B-Spline	square, cube, absolute value	32.3	No – too low	None
Rectangular Windowed Sinc $width = 7$	sinc	33.4	Yes	Grid
Hann Windowed Sinc $width = 5$	sinc, cosine	37.0	Yes	Grid
$width = 7$		39.1	Yes	None
Hamming Windowed Sinc $width = 5$	sinc, cosine	37.6	Yes	Grid
$width = 7$		38.5	Yes	None
Blackman Windowed Sinc $width = 5$	sinc, cosine	36.7	Yes	Grid
$width = 7$		38.2	Yes	None
Kaiser Windowed Sinc	sinc, square, square root, Bessel			
$a = 1.0, width = 7$		34.2	No – too low	Grid
$a = 2.0, width = 7$		35.9	Yes	Grid
$a = 3.0, width = 7$		37.4	Yes	Grid
$a = 3.0, width = 9$		40.0	Yes	Grid
$a = 4.0, width = 5$		38.5	Yes	None
$a = 4.0, width = 7$		38.2	Yes	None
$a = 5.0, width = 5$		37.7	Yes	None
$a = 5.0, width = 7$		38.6	Yes	None
Lanczos Windowed Sinc	sinc, sine			
2 lobes		38.2	Yes	Grid
3 lobes		38.8	Yes	None
4 lobes		38.5	Yes	None
Gaussian Windowed Sinc	sinc, power			
$s = 0.5, width = 7$		42.9	No – too high	Grid
$s = 1.0, width = 5$		38.6	Yes	Grid
$s = 1.0, width = 7$		37.9	Yes	None
$s = 2.0, width = 7$		36.6	Yes	Grid
$s = 2.0, width = 9$		39.5	Yes	None

3.4.1 Memory and Computational Requirements

The memory requirements for the decimation/nearest neighbor and bi-linear interpolation algorithms are minimal, because both can be implemented in place with no temporary storage required beyond that needed for the computations. The other algorithms require intermediate storage ranging from enough memory to contain a partial row or column to sufficient storage to contain a copy of the entire image, depending on the implementation chosen. This intermediate storage might require larger precision than that of the input and output image values themselves to permit sufficiently accurate computations. For example, many of the interpolation functions described in Section 3.3 require floating-point values for computations. To implement these functions in 'C' on a SUN SparcStation, four bytes of storage are needed for each intermediate value of type float, while single-byte characters can be used to store the 8-bit image pixel values. In a worst-case situation, an 8 x 8 inch fingerprint card scanned at 600 ppi would require $4800 \times 4800 \times 4 = 92,160,000$ bytes of memory, assuming 4-byte floating-point numbers.

Rescaling algorithms also vary in their computational requirements. Decimation is a very simple process requiring minimal computation, whereas some rescaling algorithms involve the use of transcendental functions or other computationally-intensive methods. Although the exact requirements depend on the implementations of the algorithms, the functions (beyond addition, subtraction, multiplication, and division) required to implement each algorithm are listed in Table 1.

3.4.2 Geometric Integrity

As illustrated in Section 4.3, an image that has been rescaled by 6:5 decimation will periodically not meet the scanner geometric accuracy requirement of the FBI's IAFIS Image Quality Specification (IQS) [FBI, 1994]. Because interpolation functions calculate rescaled pixel values based on all of the original pixels, however, the proportions of the underlying image are preserved during rescaling. The interpolation functions for image rescaling, therefore, yield acceptable geometric accuracies.

3.4.3 Qualitative Image Quality Assessment

For at least one choice of parameters for each interpolation algorithm, a composite image consisting of the rescaled sine wave targets (with Fourier transforms), the "high quality" fingerprint, and a gray patch (as indicated in Figure 3), was examined on a CRT display and assessed qualitatively. The original 600 ppi composite test image is shown in Figure 4 and Figures 5-8 show the rescaled composite test images. These images are available in their original softcopy form, see footnote 2. The fingerprint images in these composites all contain more than the 200 gray levels required by the IAFIS IQS requirement for scanner "Gray Scale Range of Image Data".

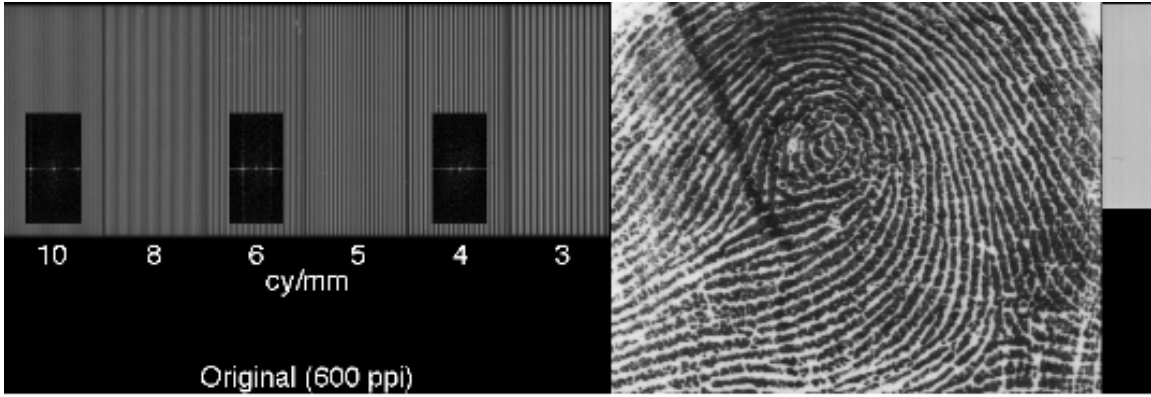


Figure 4. Original 600 ppi Composite Test Image

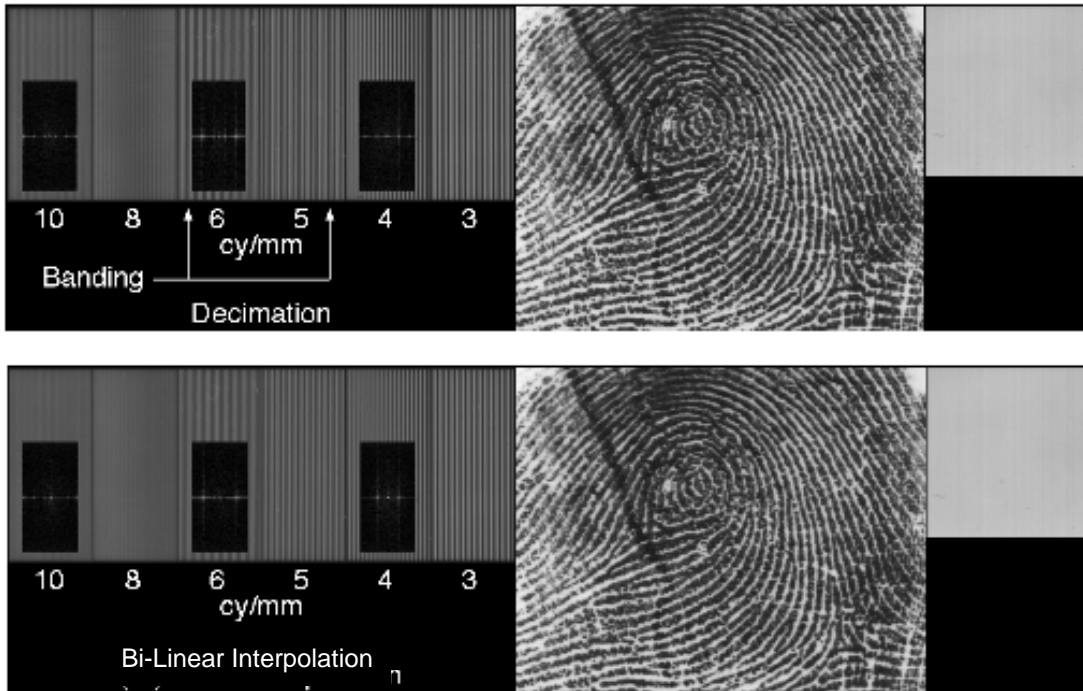


Figure 5. Composite Test Image Rescaled to 500 ppi
(Decimation and Bi-Linear Interpolation)

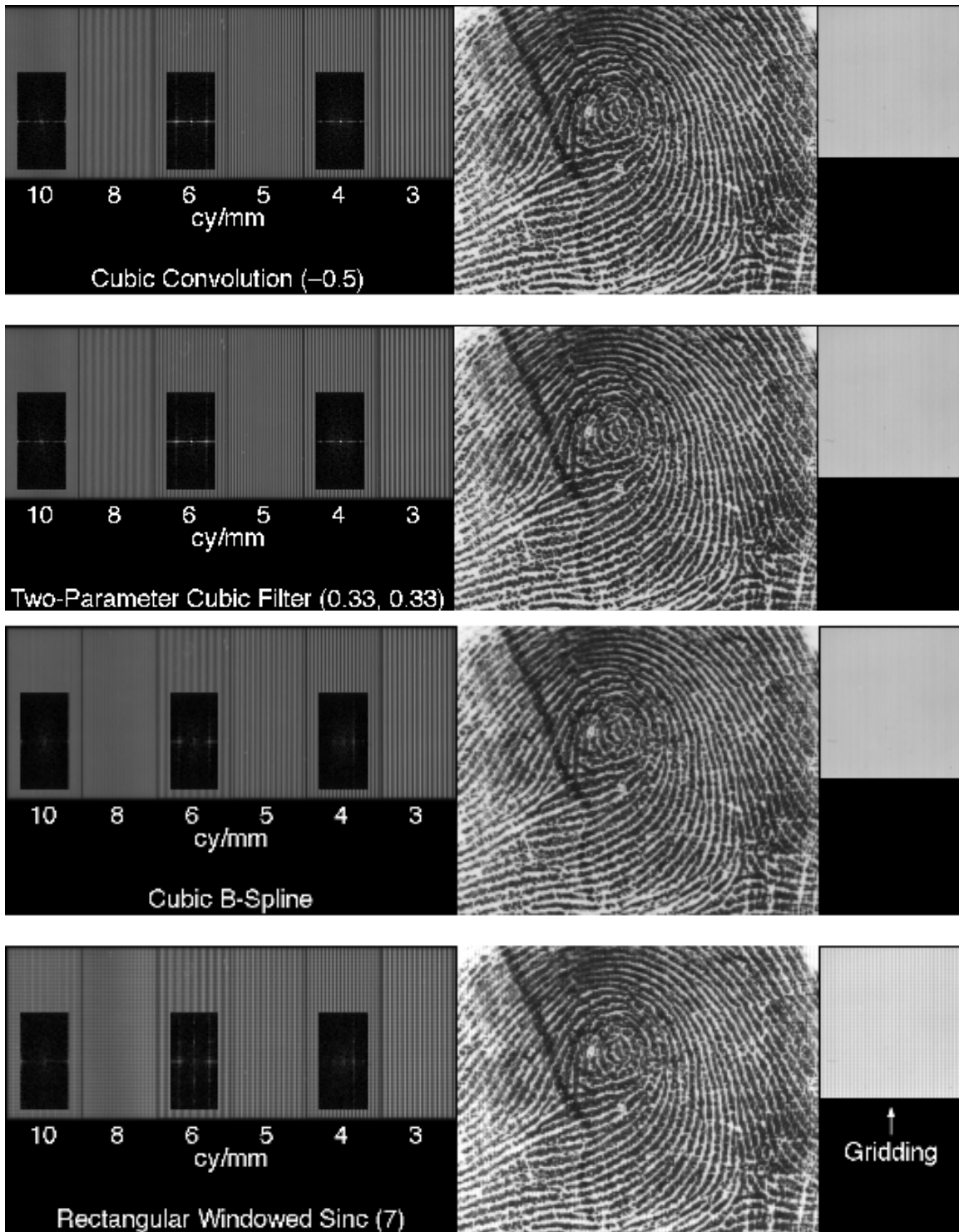


Figure 6. Composite Test Image Rescaled to 500 ppi
(Cubic Convolution, Two-Parameter Cubic Filter, Cubic B-Spline,
and Rectangular Windowed Sinc)

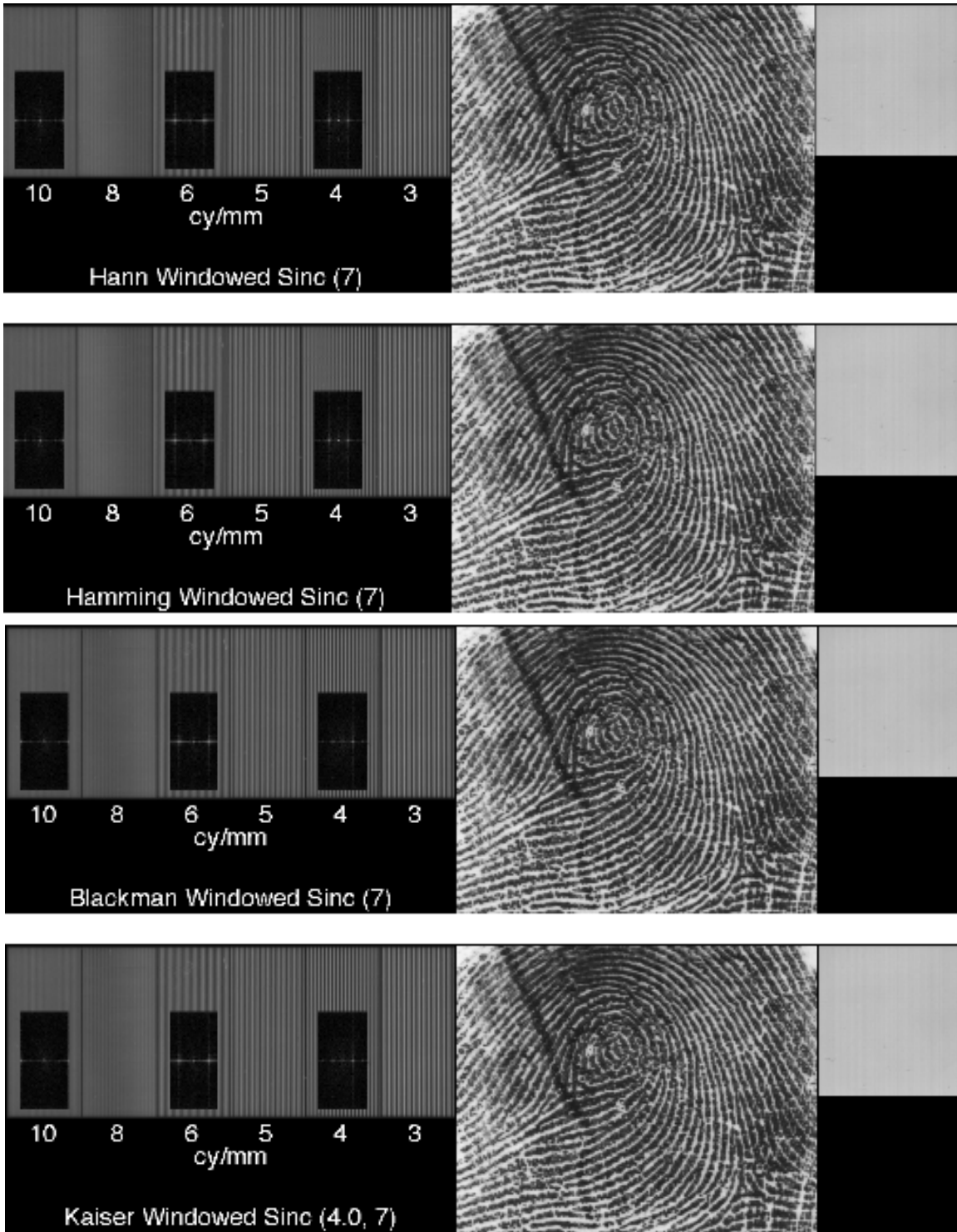


Figure 7. Composite Test Image Rescaled to 500 ppi
(Hann, Hamming, Blackman and Kaiser Windowed Sinc)

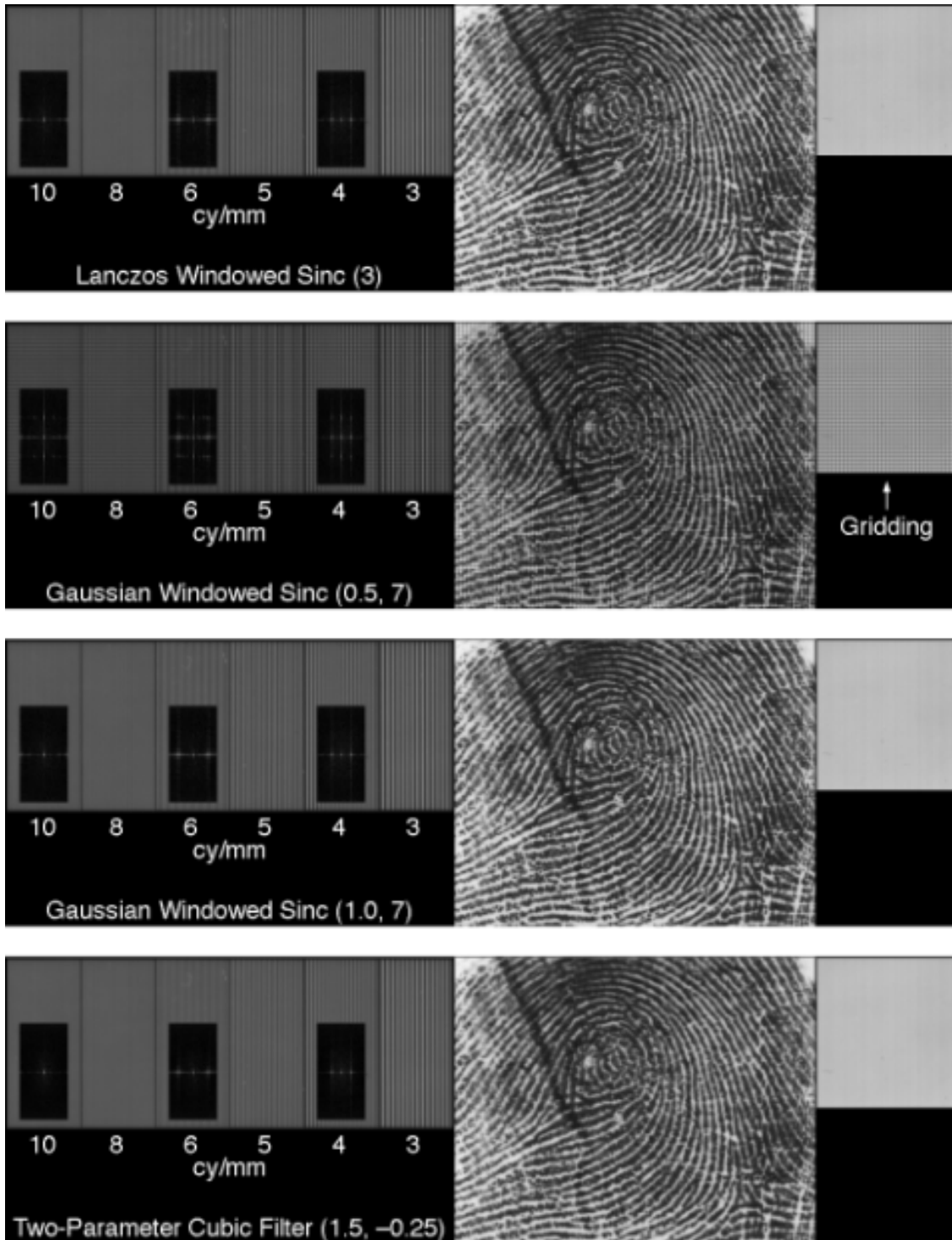


Figure 8. Composite Test Image Rescaled to 500 ppi
(Lanczos, Gaussian Windowed Sinc, and Two-Parameter Cubic Filter)

As discussed in Section 4, 6:5 decimation is nonuniform and results in abrupt shifts in the signal value. These abrupt shifts create a banding effect in the sine wave patterns that is readily apparent at certain frequencies. In Figure 5, the banding can be seen in the sine wave patterns at 6 and 5 cy/mm for decimation rescaling. The locations where the columns and rows were removed are also apparent on the decimated fingerprint image, appearing as truncated ridge edges.

An unacceptable grid pattern can occur in a rescaled image if a sinc function is applied inappropriately for image interpolation. Gridding occurs when the contributions to the interpolation of the outlying local maxima or minima of the sinc function are too strong. These strong contributions can occur for one of two reasons. First, the sinc function can be insufficiently smoothed to zero at the window edges, as can be seen in Figure 6 for the Rectangular Windowed Sinc, which has no smoothing of the sinc function. Second, the smoothing function can be too narrow to encompass enough of the local maxima and minima to balance each other out. Figure 8 shows the gridding that occurs in the Gaussian Windowed Sinc at $\sigma = 0.5$ and a neighborhood width of 7.

The effects of gridding and banding can also be seen in the Fourier transforms of the sine wave patterns. Both of these effects are exhibited by strong secondary peaks in the frequency spectra, occurring at spatial frequencies other than the sine wave's fundamental frequency. Other deficiencies in the rescaling process, as well as deficiencies in the scanner or original input, can often be detected in the frequency spectra; for example, refer back to the discussion on gray level wedging in Section 2.2.

3.4.4 Objective Image Quality Assessment of Fingerprints

One can view the hardcopy fingerprint images directly in Figures 5-8 to get a qualitative idea of the relative quality obtained by one rescaling technique versus another. A more exact comparative visual assessment can be performed with side-by-side viewing of the original images on a CRT display. A good *objective* image quality measure, however, could rank fingerprints at a finer level than is possible with visual assessments, and without the variability inherent in subjective visual assessments. To this end, an image quality measure (IQM) previously developed by MITRE [Nill and Bouzas, 1992] was applied to these fingerprint images, with the results shown in Table 1. This image quality measure is based on a summation of energy in an image's weighted, normalized power spectrum, where the power spectrum equals the squared magnitude of the FFT of the digital fingerprint, specifically:

$$IQM = \frac{1}{M^2} \sum_{\theta=-\pi}^{\theta=\pi} \sum_{\rho=0.01}^{\rho=0.5} S(\theta_l) W(\rho) A^2(T\rho) P(\rho, \theta)$$

where,

M^2 = digital image size in pixels

$S(\theta_l)$ = directional image scale parameter (constant for this application)

$W(\rho)$ = modified Wiener noise filter

$A^2(T\rho)$ = MTF² of human visual system (T =constant)

$P(\rho, \theta)$ = normalized image power spectrum

ρ, θ = spatial frequency in polar coordinates

($\rho = 0.5$ cycles per pixel width = Nyquist frequency)

For this application, the IQM (version 4.2) was applied to a 256 x 256 pixel subimage region encompassing the core of each rescaled image of the "high quality" inked fingerprint (refer to Figure 3). This IQM was originally developed and optimized for military aerial reconnaissance imagery and was applied to these fingerprint images "as is". Optimization of this IQM for fingerprints potentially could include a number of modifications, such as weighting different areas of the print (e.g., more weight to core area), adjusting the noise filter parameters and human visual system filter peak location, determining/incorporating differences between quality for visual evaluation versus machine evaluation (e.g., AFIS), and modifying the current artifact detectors for fingerprint artifacts.

To first order, the IQM rates quality as a function of image blur or edge sharpness. The less blur or the sharper the edges, the more high frequency content in the power spectrum, resulting in a higher quality rating. Thus, it is no surprise that one of the highest quality ratings was obtained from the 6:5 decimation rescaling case (IQM = 39.2), because this image retains the frequency content and sharpness of the original 600 ppi image scan, whereas the other 6:5 interpolation techniques smooth ("blur") the image to varying extents. The IQM does not currently separate out aliased energy appearing below the Nyquist frequency, so this energy adds to the non-aliased energy. Since the decimation case has the strongest aliased energy, it also adds to the quality rating magnitude for this case. The grid pattern exhibited in some of the interpolation images (noted under "artifacts" in Table 1) also creates false power spectrum energy which adds to the respective images' quality ratings. However, since the decimation and interpolation-with-grid-pattern result in unsatisfactory fingerprint images, these are discarded from the set evaluated with respect to the IQM.

In Table 2, the IQM is compared to visual quality assessments for the remaining 18 interpolation cases corresponding to satisfactory fingerprint images. The objective IQM tracks the visual assessment of quality obtained from side-by-side viewing on a CRT display. In fact, the visual assessments (albeit by a non-fingerprint expert) can do no better than bin the images into one of three general quality levels.

Table 2. Objective and Subjective Assessments of Fingerprint Image Quality

Interpolation Technique (parameter values)	Objective Quality (IQM)	Subjective Quality Assessment
Cubic Convolution (-1.0)	40.7	BEST
Gaussian Windowed Sinc (2.0, 9)	39.5	
Cubic Convolution (-0.75)	39.4	
Hann Windowed Sinc (7.0)	39.1	
Lanczos Windowed Sinc (3.0)	38.8	
Kaiser Windowed Sinc (5.0, 7)	38.6	
Lanczos Windowed Sinc (4.0)	38.5	
Kaiser Windowed Sinc (4.0, 5)	38.5	
Hamming Windowed Sinc (7.0)	38.5	
Kaiser Windowed Sinc (4.0, 7)	38.2	
Blackman Windowed Sinc (7.0)	38.2	
Cubic Convolution (-0.5)	38.1	
Gaussian Windowed Sinc (1.0, 7)	37.9	
Kaiser Windowed Sinc (5.0, 5)	37.7	
Two-Parameter Cubic Filter (0.33, 0.33)	36.0	MEDIUM
Bi-Linear Interpolation	35.7	WORST
Cubic B-spline	32.3	
Two-Parameter Cubic Filter (1.5, -0.25)	29.9	

(‘No-artifact’ interpolation rescaling cases.)

The IQM values measured from the fingerprint images are also in agreement with the MTFs measured from the sine wave images, as shown in Figure 9. Thus the power spectrum-based image quality measure can be usefully applied to the objective assessment of fingerprint quality.

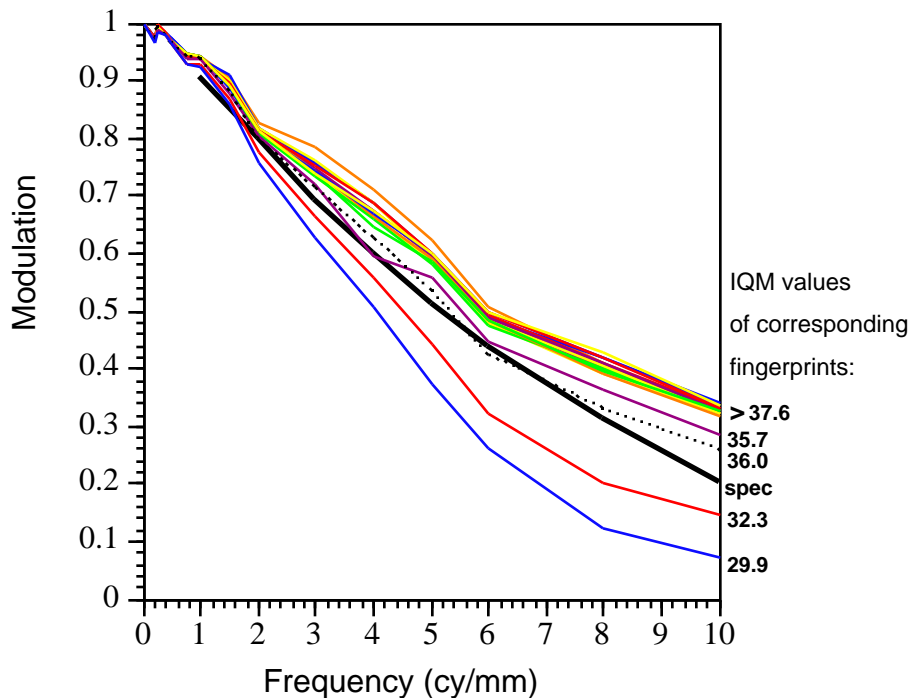


Figure 9. MTFs Associated with Interpolation Methods Not Exhibiting Visual Artifacts

3.4.5 Objective Image Quality Assessment via MTF

The MTF computed from the 500 ppi rescaled sine wave targets must fall within specified ranges at certain frequencies, as described in the FBI's IQS requirements for fingerprint scanners [FBI, 1994]. The MTF was computed from the 500 ppi sine wave images as rescaled by each of the interpolation algorithms, using the MITRE-developed sine wave MTF computer program [Nill and Paine, 1994], version 2.2. The results of these tests are reported in Table 1. Figure 9 shows the MTFs associated with the 18 interpolation methods that did not exhibit visual artifacts; all but two of which meet the IAFIS IQS scanner MTF requirement [exceptions: *cubic B-spline* and *two-parameter cubic filter* (1.5, -0.25)].

As listed in Table 1 and shown graphically in Figure 10, most of the 13 interpolation methods that do exhibit unsatisfactory visual artifacts (gridding or banding), also are within the upper and lower bounds of the spec MTF. For the interpolation gridding cases, this is partly due to the fact that the MTF analysis program performs some amount of noise filtering (e.g., by row averaging). When such visual artifact cases occur, however, either the "signal to noise ratio" or the "output gray level uniformity" IQS scanner requirement will most likely not be met. Also, as discussed in Section 6.2, implementation of a robust alias/artifact detector would flag these unsatisfactory cases.

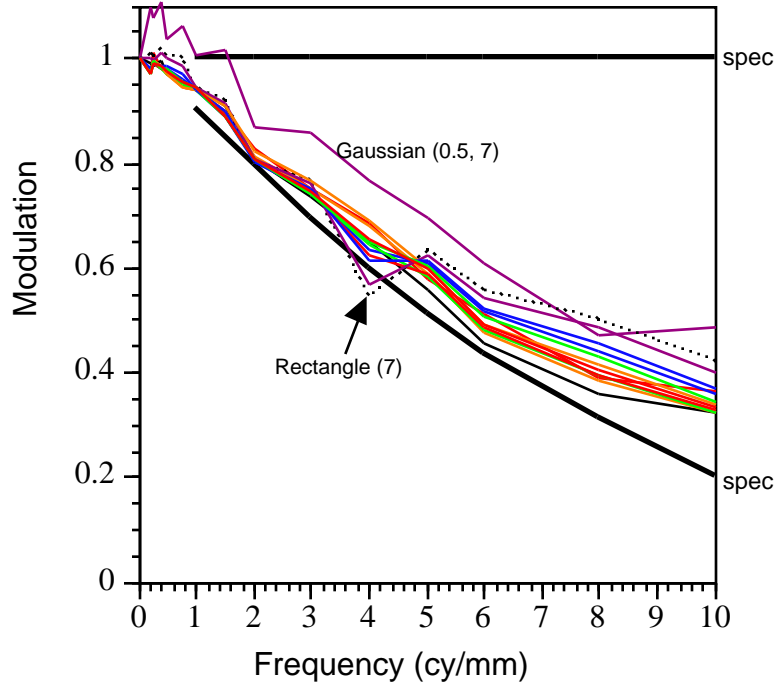


Figure 10. MTFs Associated with Interpolation Methods Exhibiting Visual Artifacts

3.5 Implementation Details

Although the interpolation functions described in Section 3.3 can be implemented in a straightforward manner, certain considerations should be kept in mind to yield satisfactory results while minimizing the computation and storage required.

Several of the functions described can produce pixel values that lie outside the range of values found in the original image. For these functions, the output values must be limited to the appropriate range. For all methods (except nearest neighbor and decimation), floating point results must be rounded or otherwise converted to integer values for the final output image.

One possible implementation of the 1-D interpolation functions is *Fant's resampling algorithm*, which is described by [Wolberg 1992, page 153]. This, or a different implementation, can be used to pass the 1-D functions horizontally, then vertically (or vice versa) over an image to rescale it.

With a rescaling from 600 ppi to 500 ppi, the output image will be smaller than the input image. Therefore, if separate horizontal and vertical processing steps are implemented, it is possible to store the intermediate results back into the original image space after processing each full row or column. However, better results may be obtained if the

precision of the intermediate results is higher than that of the original image. In this case, more space for the storage of intermediate results is required.

Because each interpolation function mentioned above has limited extent, neighborhood row and column passes can be performed to determine each output pixel. With this sort of implementation, no intermediate storage is required for full image rows or columns, but storage is required for the square neighborhood that the function covers and for the output image. [The algorithm cannot overwrite the input values as the output values are determined because the input values are needed in a neighborhood around each output value to be calculated.]

Most of the methods described above use pixel values on either side of an output pixel to determine its value. There is then the question of what should be done at the image edges. If the pixel values at the edges of the input image are replicated as needed by the interpolation function being applied, then the output image will change smoothly near the edges. If zeros are instead assumed outside of the input image bounds, a harsh edge effect may be exhibited.

For sinc-based and sinc-like interpolation functions, the choice of extent of the function is important. For most of the functions, a width of $n = 5$ can yield uneven results in smooth portions of the image due to large contributions from the first side lobes of the sinc, which are negative. Higher values of n tend to ameliorate this effect, though the choice of n depends on the interpolation function being used.

Some of the interpolation kernels require rather intensive computations. However, for a given choice of input and output resolutions, there are a finite number of kernel values, which repeat. These repeated values can be calculated once and stored for use as needed. For example, if the input resolution is 600 ppi and the output resolution is 500 ppi, then the interpolation function values in a row or column will repeat every 5 output pixels. This is easy to see when one notes that the initial output pixel is in exactly the same position as the initial input pixel. There are a total of five distinct function positions before the pattern repeats with the input and output pixels being once again aligned.

3.6 Conclusions

Many interpolation algorithms are available for rescaling an image, and a number of these were explained and evaluated in this section. It has been demonstrated that parameter settings for an algorithm that result in the appearance of a grid in the rescaled output are not acceptable. Also, any algorithm resulting in an MTF that falls significantly outside the IAFIS IQS requirements range is not acceptable. Certain specific algorithms are also deficient. Decimation/nearest neighbor rescaling, because of the banding effect obvious in the sine wave targets, is not satisfactory. Two interpolation functions, the cubic B-spline and the two-parameter cubic filter with $b = 1.5$ and $c = -0.25$, fall clearly below the MTF requirement range. Gaussian windowed sinc interpolation with $s = 0.5$ exhibits gridding at any neighborhood width because the Gaussian window is too narrow. The suitability of other algorithms depends on the choices of parameters used to implement them. The

parameter choices, in turn, depend on design trade-offs in hardware and software, so no one algorithm can be deemed best for all situations. Often, an algorithm will not be acceptable with one set of parameters, but will be acceptable with another. The MTF of the algorithm, the visual quality of the output, and memory and computational requirements must all be considered when choosing a rescaling algorithm. The basic conclusion, however, is that there are a number of viable interpolation techniques that can be applied to downward rescaling of fingerprints which result in IAFIS-acceptable images.

SECTION 4

RESCALING DOWNWARD IN RESOLUTION VIA DECIMATION (NEAREST NEIGHBOR)

Decimation reduces the size and resolution of an image by simply removing rows and columns of pixels; it is therefore limited to rational number size reductions. For example, a two-to-one decimation (denoted in this document as 2:1) removes every other row and every other column, producing an image that is half the size. Decimation is often utilized in downward rescaling because it is the simplest rescaling technique, with almost no computational burden or extra computer memory requirements. *Nearest neighbor* rescaling is equivalent to decimation, the only difference is in the specific rows and columns that are removed to reduce the size and resolution. As will be seen in this section, however, the type of decimation that would most likely be applied to rescale to 500 ppi, known as nonuniform decimation (e.g., rescaling from 600 ppi to 500 ppi), results in unsatisfactory fingerprint images.

4.1 UNIFORM DECIMATION

There are actually two types of decimation that have drastically different effects on the quality of the down-sampled signal.

The first, well understood type is *uniform decimation*, for which the decimation is achieved by keeping every Mth sample of a signal. Examples of this type of decimation is 2:1, where every other sample is retained in the resampled signal, and 3:1, where every third sample is retained. All uniform decimations can be reduced to the annotation form M:1 decimation, where M is an integer, by dividing both sides of the colon by the same value, e.g., 500:250 decimation reduces to the 2:1 decimation case by dividing both sides by 250. This type of decimation can be simply modeled as having sampled the signal at the resolution desired in the first place. The fact that extra samples were collected originally has no effect on the resulting resampled signal, except that there may be a difference due to the pixel integration size of the sampling system. Typically, the decimated signal will appear sharper than a signal produced by the lower resolution system at the desired sampling rate due to the effectively smaller pixel size of the higher resolution system. Uniform decimation does not cause aliasing or other adverse effects on image quality, but it is limited to those cases of decimation that can be reduced to the form M:1, such as 1000 ppi to 500 ppi, or 500 ppi to 250 ppi decimation.

4.2 NONUNIFORM DECIMATION

In order to achieve 500 ppi from a 600 ppi scanner by decimation, however, the second type of decimation, termed *nonuniform decimation*, is required. Nonuniform decimation, where every Mth pixel is removed (rather than retained) from the original signal, does have objectionable properties with respect to image quality. Decimation of this type can

be denoted as M:N decimation, where $M=N+1$ (e.g., 6:5 decimation)³. Nonuniform decimation produces the desired number of samples per signal length, but the decimated signal actually consists of bands of the signal sampled at the higher resolution, interrupted by abrupt shifts in the signal. Figure 11 illustrates a 6:5 decimation on a sampled sine wave. In this decimation, groups of five samples, spaced apart by one sample, are expanded and shifted together to yield the new digital waveform. Notice that the new digital waveform does not closely match the overlaid original sine wave. This is primarily caused by the abrupt shifts of the signal data values and the fact that the samples were originally taken at the 600 ppi resolution within each group of five.

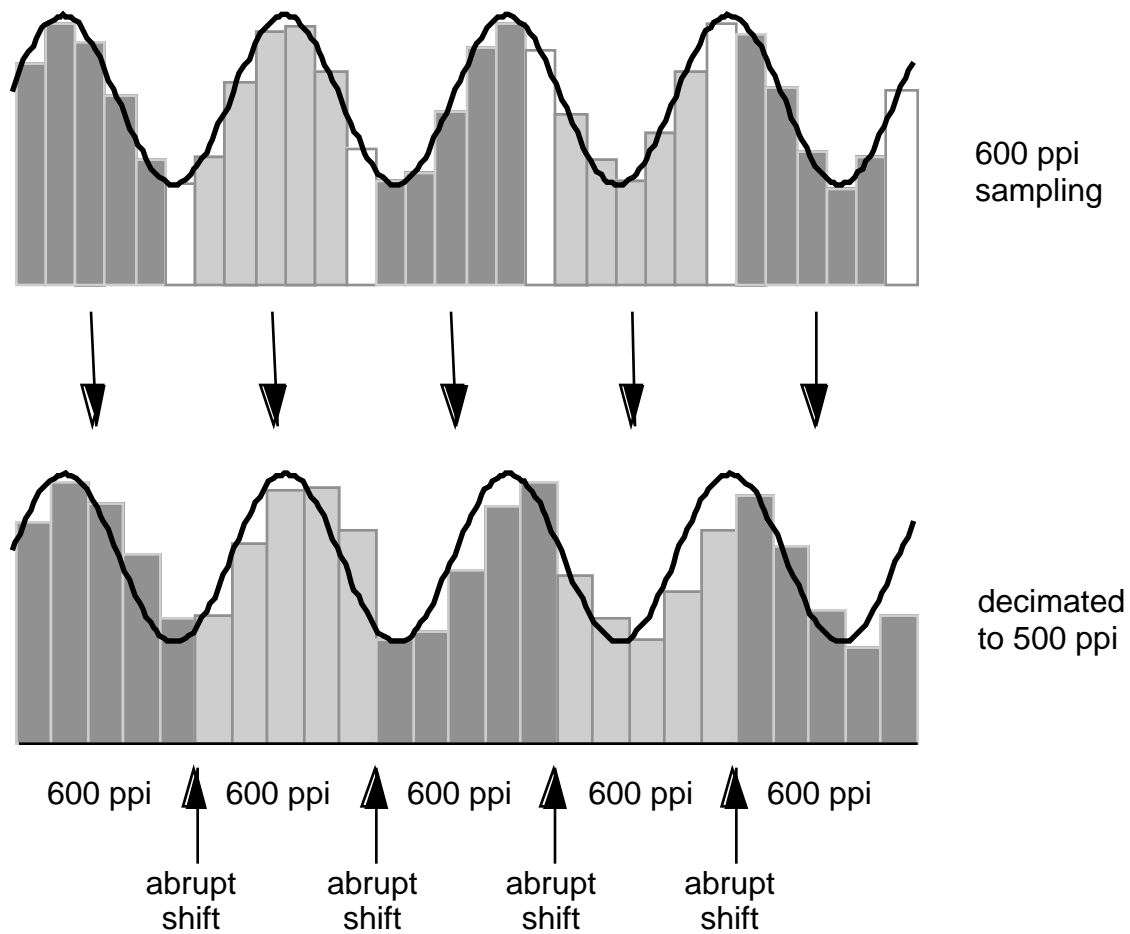


Figure 11. Pixel Locations of Sine Wave Image Decimated from 600 to 500 ppi

When decimation is applied to image data, it is applied independently in the row and the column directions. In the case of 6:5 decimation, 5x5 pixel blocks are shifted together by one pixel in both directions, resulting in a grid of abrupt shifts. However, the visibility of

³ Categorizing decimation into two types, uniform and non-uniform, is a useful construct for most cases. Note, however, that 2:1 decimation can fit either definition type. In practice, 2:1 decimation should be categorized as uniform decimation, with its corresponding lack of image quality degradation.

these abrupt artifacts is dependent on the image content. Although the abrupt shifts are not apparent in high contrast, horizontal and vertical edges, they are visible as “staircasing” on diagonal edges. Figure 12 compares the effect of 6:5 decimation to 6:5 bi-linear interpolation of a tribar target scanned at 600 ppi on an Eikonix model 1412 scanner. In the interpolated case the image is smooth with no abrupt changes, but in the decimated case the abrupt shifts can be seen on the diagonal segments of the numbers in the target. The decimated case has a sharper appearance than the interpolated case, but it is because its local resolution is actually 600 ppi. These results are in agreement with initial experimentation on the subject reported awhile ago at MITRE [Hwang, 1993].

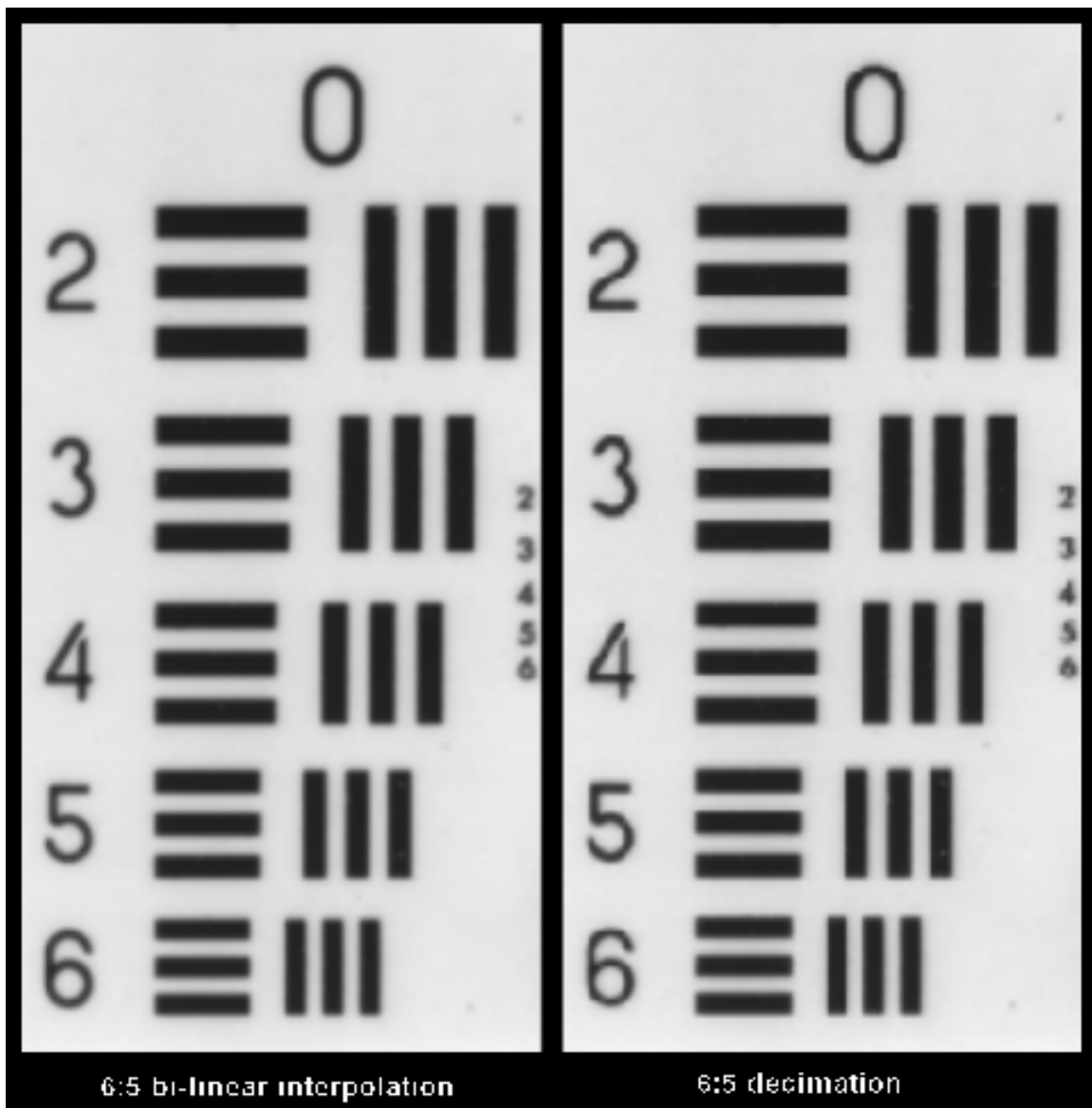


Figure 12. 600 ppi Tribar Scan Rescaled to 500 ppi via Bi-Linear Interpolation and Decimation

Referring back to Figures 2 and 5, it was seen that nonuniform decimation causes strong secondary peaks in the Fourier spectra of sine waves, which is indicative of aliasing. To further characterize the aliasing effects resulting from nonuniform decimation, a series of pure digital sinewaves of specified frequencies and sampling resolutions was constructed, and the Fast Fourier Transform (FFT) was then applied to these constructions. Decimation was then simulated by dropping every Mth sample prior to the FFT. The details of this analysis are given in Appendix B. The analytical approach in Appendix B confirms the experimental results illustrated in Figures 2 and 5; i.e., that nonuniform decimation causes strong harmonics (secondary peaks) to appear in the frequency spectra. These harmonics are a characteristic of aliasing, which causes artifacts to appear in the image itself.

4.3 DECIMATION EFFECT ON GEOMETRIC ACCURACY

The rescaling technique of 6:5 decimation may result in the IAFIS IQS requirement for scanner geometric accuracy not being met. The measurement of scanner geometric accuracy is affected because the decimation will nonuniformly change the edge locations of the Ronchi ruling bars of the test target used to verify IAFIS IQS compliance. The test target uses 0.500 mm wide Ronchi ruling bars spaced apart by 0.500 mm (1 cy/mm Ronchi). At 500 ppi, the distance between consecutive bar centers would be 19.685 pixels for perfect geometric accuracy. In the case of a 600 ppi image reduced to 500 ppi by 6:5 decimation however, the measured bar center-to-bar center distance can range between 19.600 and 20.167 pixels, as illustrated in Figures 13 and 14.

The geometric accuracy requirement will not be met for a portion of the measurements because the error caused by decimation is greater than the allowed $\pm 1/3$ pixel error (e.g., $20.167 - 19.685 = 0.482$ pixel error). The impact of this error is variable, however, because not every area of every print block is tested, because the error is location-dependent, and because 99% (not 100%) of all cases tested within a print block need to meet the $\pm 1/3$ pixel error limit. Although the Ronchi target is also used to verify scanner resolution, the measurement error due to decimation will be small compared to the relatively large distance measured (0.4 to 1.25 inches), with the result that decimation should not adversely affect the ppi resolution measurement.

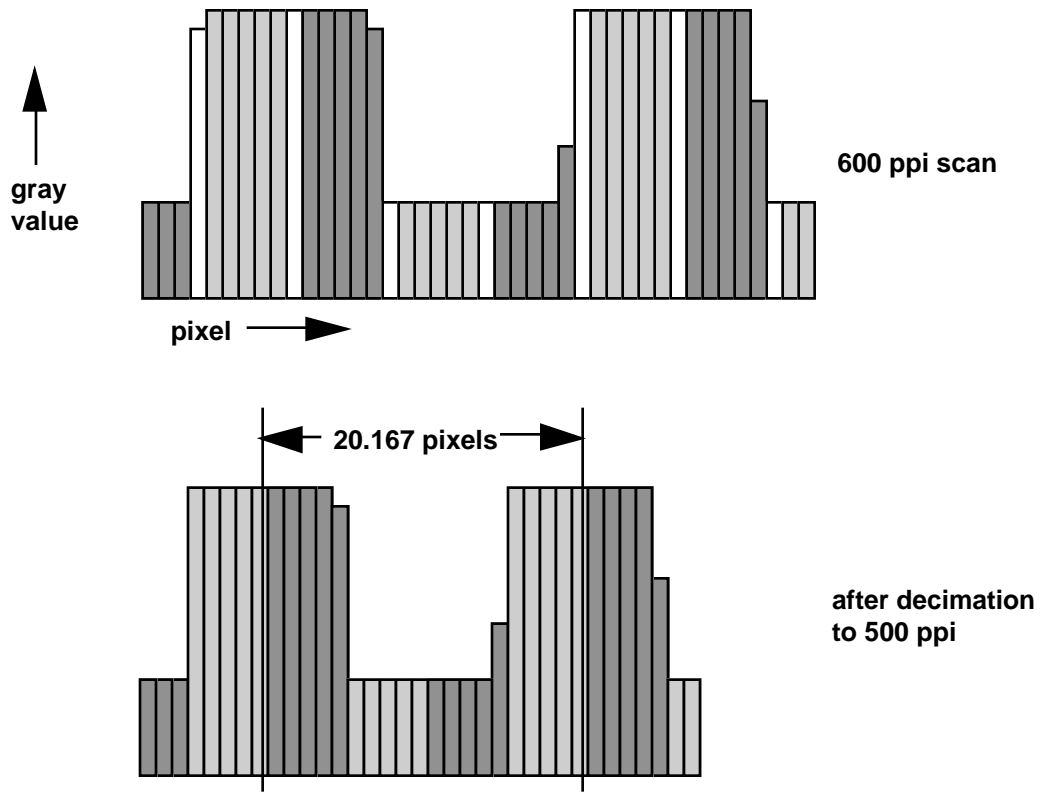


Figure 13. Decimation Applied to a Pair of Ronchi Bars That Causes Maximum Separation

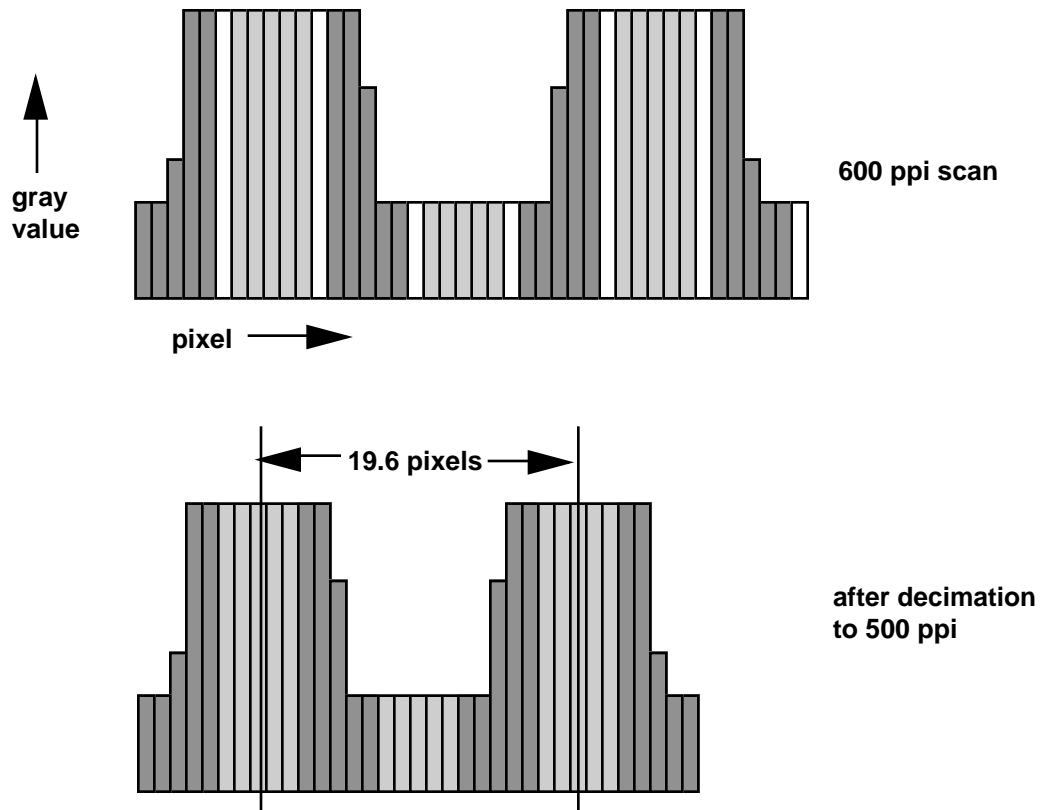


Figure 14. Decimation Applied to a Pair of Ronchi Bars That Causes Minimum Separation

4.4 IMPLICATIONS

Nonuniform decimation, such as decimation from 600 to 500 ppi, produces visible aliasing-like artifacts. It needs to be determined through experimentation if these artifacts are strong enough to significantly affect visual fingerprint matching, the performance of an Automated Fingerprint Identification System (AFIS), or the performance of the IAFIS Wavelet Scalar Quantization (WSQ) fingerprint compression algorithm. It would not be surprising to find that the discontinuities caused by decimation adversely interact with AFIS minutia detection algorithms or a transform-based lossy compression technique such as WSQ, which is more tuned to operating on smooth surface input images. Concerning the latter, we ran a small experiment which does indicate that there is a visibly adverse interaction between nonuniform decimation and WSQ.

The occurrence of image artifacts, coupled with the fact that nonuniform decimation can result in the IAFIS IQS geometric accuracy requirement not being met, indicates that this rescaling technique is, at best, only marginally acceptable. Since various interpolation rescaling techniques can be relied upon to consistently give acceptable image quality and are not difficult to implement, there is no reason to take a gamble on nonuniform decimation when rescaling is implemented.

SECTION 5

RESCALING UPWARD IN RESOLUTION

A number of commercial scanners have a true resolution, sometimes referred to in their literature as "optical resolution", of 300 or 400 ppi. These scanners can output a higher, user-selected resolution, such as the IAFIS-required 500 ppi, by applying upsampling rescaling algorithms to the scanned image. However, although an upward rescaled image may be 500 ppi in a geometric sense, no upward rescaling processing method will completely meet the IAFIS MTF requirement for image quality. Upward rescaling invariably produces aliasing, which exhibits itself in the image as false information, which results in unacceptable image quality.

To illustrate this important point, the MTFs were measured from the 300 to 500 ppi rescaled sine target images that are partially shown in Figure 2 as *Eik3* and *Eik4*, corresponding to replication (the opposite of decimation) and bi-linear interpolation rescaling, respectively. [It is known that the Eikonix scanner, when operating at a true 500 ppi, does meet the IQS MTF requirement.] The sine target was also scanned on a Mitsubishi SC-7500 flatbed scanner, which has a true resolution of 400 ppi, and the MTF was then measured from the Mitsubishi output image rescaled to 500 ppi via replication and via cubic convolution interpolation. [Cubic convolution interpolation is one of the better interpolation techniques discussed in Section 3 (parameter value = -1.0).] The MTF results are shown in Figure 15, where it is seen that the 3:5 rescale cases fall far below the IQS minimum acceptable MTF curve.

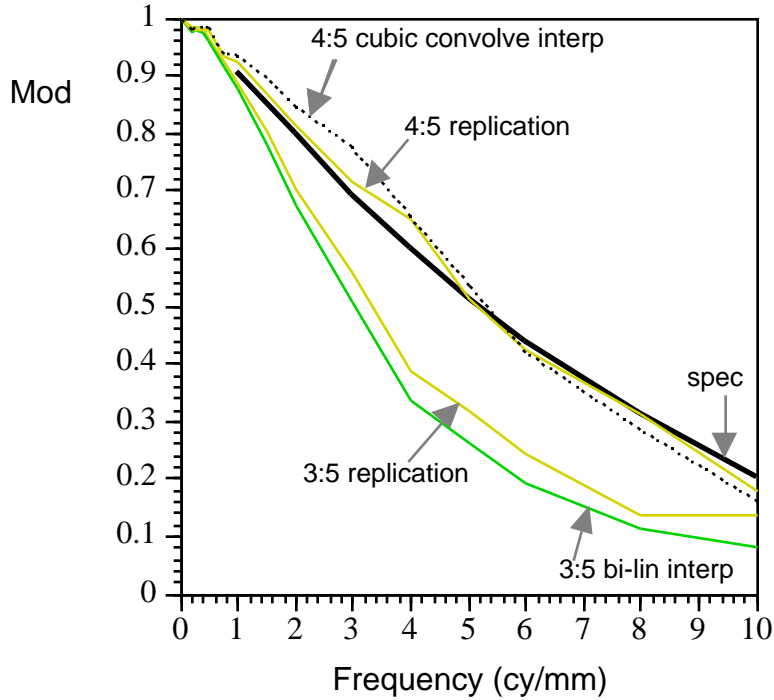


Figure 15. MTFs of 300 and 400 ppi Scanners Rescaled Upward to 500 ppi

For the case of 4:5 rescaling via replication, however, the computed MTFs in Figure 15 almost meet the minimum acceptable MTF; the computed MTF of a higher quality 400 ppi scanner could conceivably meet it. However, the measured MTF would only meet or nearly meet the minimum acceptable MTF because the aliasing present causes frequency spectrum energy to be rearranged, resulting in a pure sine wave (at 400 ppi) becoming a sine wave with harmonics (at 500 ppi). [Aliasing in this context is described further in Appendix B.] The logic of the MTF software assumes the pattern being measured is a pure sine wave, whereas the presence of harmonics will alter the peak and valley values of the measured sine wave. In these cases, the computed MTF curve must be taken together with observations of the rescaled sine pattern images and their Fourier spectra, and/or taken together with alias detection algorithmic results, to get a complete picture. This was done for the 4:5 rescaling case with the results summarized in Table 3.

Table 3. Multi-Factor Analysis of Upward Rescaling of Sine Waves

Factor:	4:5 Rescaling via Replication	4:5 Rescaling via Cubic Convolution Interpolation
MTF	~ meets spec	below spec
Aliasing*	8 & 10 cy/mm	8 & 10 cy/mm
Visual - Sine Patterns	significant banding down to 5 cy/mm	no banding
Visual - FFT of Sine Patterns	strong secondary peaks down to 4 cy/mm	secondary peak at 10 cy/mm

* as detected by the 'alias detector' in the MITRE sine MTF software version 2.2.

Table 3 indicates that 4:5 rescaling, either by replication or by cubic interpolation, does not meet the *total* MTF requirement, which requires *both* a minimum acceptable modulation at each frequency (as specified in the IQS) and no aliasing (as specified in the IQS Test Procedures). Visual assessment is good confirmation of these quantitative results.

The unacceptability of upward rescaling also applies to the IAFIS 1000 ppi latent print scanner. This is particularly worth noting because there are a number of commercial scanners on the market today that advertise "1200 ppi resolution", when in fact they have a true resolution of 600 ppi and use interpolation to obtain 1200 ppi [this fact is sometimes noted in the fine print, and sometimes not]. Scanning at 600 ppi and rescaling to 1000 ppi by interpolation would give equivalently poor results as that illustrated in Figure 15 for the 300-to-500 ppi case.

SECTION 6

IDENTIFYING AND DETECTING RESCALING

6.1 IDENTIFYING A GOOD RESCALING TECHNIQUE FOR IMPLEMENTATION

For those responsible for implementing a scanner rescaling technique, a good technique can be identified when the 500 ppi rescaled image exhibits the following properties:

- 1) There is no visible gridding on uniform gray areas. Correspondingly, IQS requirements for signal to noise ratio and gray level uniformity are met.
- 2) The rescaled image meets the complete scanner MTF requirement in the IAFIS IQS. Implicitly, the original, unscaled image output from the scanner (e.g., 600 ppi image) would also need to meet the MTF requirement.
- 3) No banding is visible on the rescaled sine wave images, indicating no excessive aliasing. Correspondingly, the intensities of secondary energy spikes in the Fourier domain would have to be 'small', relative to the energy spike at the sine wave fundamental frequency. Aliasing should not be detected by the MTF analysis software, at any frequency up to and including the Nyquist frequency.
- 4) The computational load and memory requirements of the technique must be compatible with the given computer hardware/software system utilized, and the total system must meet operational performance requirements.
- 5) The geometric integrity must meet the IQS geometric accuracy requirement.

6.2 DETECTING THE PRESENCE OF AN UNACCEPTABLE RESCALING TECHNIQUE

For those responsible for testing scanners, the visual appearance of gridding, banding, or secondary spikes in the Fourier domain is a useful qualitative method for assessing the suitability and acceptability of the rescaling, without actual knowledge of the technique used to produce the images. These visual checks, along with the MTF measurement itself, can be made with the IAFIS IQS-specified sine wave target.

It is entirely possible, however, for the MTF range requirement to be met, and at the same time, for the visual assessment results of the sine image to be ambiguous, improperly interpreted, or not interpreted at all. For example, in the case considered in Table 3 for 4:5 rescaling, a better 400 ppi scanner using cubic convolution interpolation rescaling could conceivably meet the minimum acceptable MTF and would not show any visible signs of banding. Also, visual assessment of the sine patterns in the Fourier domain would show nothing out of the ordinary or would be ambiguous. In such a case, only quantitative,

objective, unambiguous assessment could detect the unacceptability of the rescaling technique.

A partial solution to this objective assessment problem is incorporated in the MITRE-developed sine wave MTF computer program [Nill and Paine, 1994, section 2.8]. The alias detector in this program (versions 2.1 and 2.2) calls out the presence of aliasing if the maximum peak in a given sine pattern's Fourier spectrum occurs at the wrong frequency. The logic of this algorithm will detect cases of rescaling upward in resolution, such as the 400 to 500 ppi case, as demonstrated in Table 3. Measurements on downward rescaling (e.g., 600 to 500 ppi), however, indicate that for these cases secondary peaks in the Fourier spectra are *not* as strong as the peak at the correct frequency location (not usually or not ever - to be resolved). The result is that the current alias detection algorithm does not detect downward rescaling. To consider these cases, and also detect such artifacts as 'gridding' caused by selection of the wrong interpolation parameter values, a more widely applicable detector is needed, can be developed, and should be implemented.

REFERENCES

- Bracewell, R., 1965, *The Fourier Transform and Its Applications*, McGraw-Hill, New York, pp. 189-194.
- Crochiere, R. E. and L. R. Rabiner, 1983, *Multirate Digital Signal Processing*, Prentice-Hall, Englewood Cliffs, NJ, pp. 31-42.
- FBI, 1994, *Electronic Fingerprint Transmission Specification*, Appendix F, "IAFIS Image Quality Specifications (IQS)", document number CJIS-RS-0100 (V3), Federal Bureau of Investigation, Washington, DC.
- Gori, F. and G. Guattari, 1971, *Non-Uniform Sampling in Optical Processing*, *Optica Acta*, Vol. 18, No. 12, pp. 903-911.
- Hwang, V.S., 3 November 1993, *MTF and Perceived Image Quality*, MITRE Memo J071-M-271 (3468C), The MITRE Corporation, McLean, VA.
- Null, N.B. and B. R. Paine, September 1994, *A Computer Program to Determine the Sine Wave MTF of Image Scanners*, MITRE Technical Report MTR-94B36, The MITRE Corporation, Bedford, MA.
- Null, N.B. and R.D. Forkert, 9 January 1995, *Recommended MTF Specs for 1000 ppi and 250 ppi Scanners*, MITRE Technical Letter G034-L-022, The MITRE Corporation, Bedford, MA.
- Null, N.B. and B.H. Bouzas, April 1992, *Objective Image Quality Measure Derived from Digital Image Power Spectra*, *Optical Engineering*, Vol. 31, No. 4, pp. 813-825.
- Nordbryhn, A., 1983, *Sampling and Aliasing Problems with Imaging Arrays*, *Proceedings of Photo-Optical Instrumentation Engineers*, SPIE vol. 467, "Image Assessment: Infrared and Visible (SIRA)", pp. 116-121.
- Schreiber, W.F. and D. E. Troxel, March 1985, *Transformations Between Continuous and Discrete Representations of Images: A Perceptual Approach*, *IEEE Trans. Pattern Analysis and Machine Intelligence*, Vol. PAMI-7, No. 2, pp. 178-186.
- Wolberg, G., 1992, *Digital Image Warping*, IEEE Computer Society Press, chapter 5, "Image Resampling", Washington, DC. An errata sheet can be obtained by contacting the author at Columbia University via email: wolberg@cs.columbia.edu

APPENDIX A

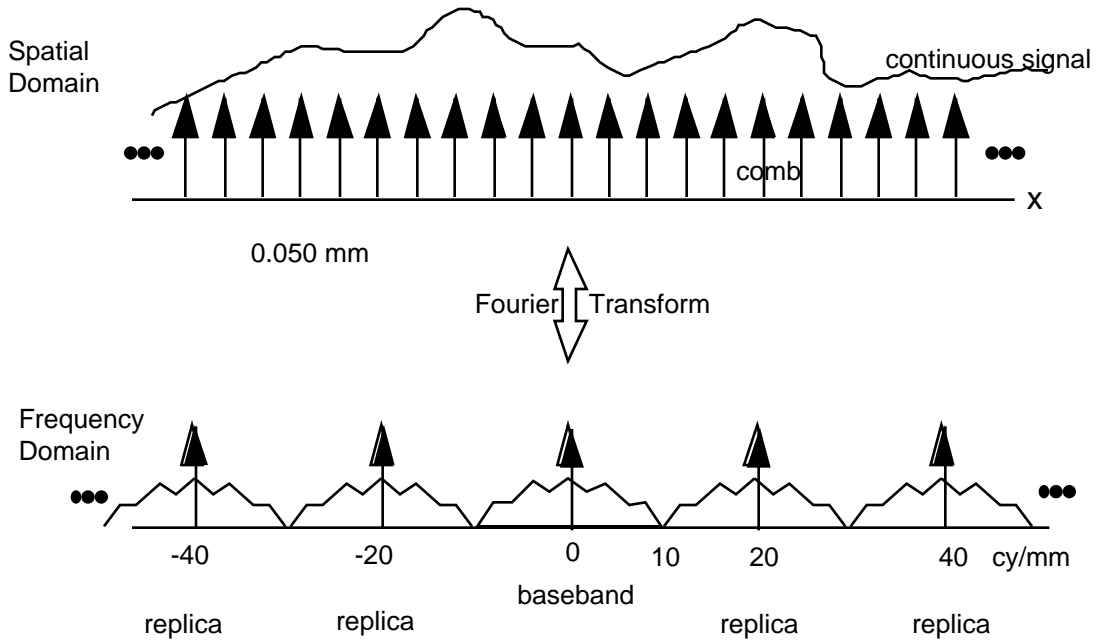
SAMPLING THEORY VIEW OF ALIASING

According to sampling theory, two basic conditions must be met in order to correctly sample a continuous signal without producing aliasing. First, the signal must be bandlimited. This means that the frequency content of the signal must be zero for all frequencies higher than a specified frequency, f_{nyq} . Second, the sampling interval, Δ , applied to the signal must be less than or equal to $1/(2f_{nyq})$. The frequency f_{nyq} is known as the Nyquist frequency, which is equal to $1/(2\Delta)$.

Point sampling of a continuous signal can be modeled by multiplying the continuous signal by a periodic train of impulse functions called the comb function [Bracewell, 1965]. If two functions are multiplied in the space domain, then the equivalent operation performed between the Fourier transforms of the two functions is convolution; thus the Fourier transform of the continuous signal is convolved with the Fourier transform of the comb function. As it turns out, the Fourier transform of a comb function is just another comb function, but with reciprocal spacing of the impulse functions making up the transformed comb function. Modeling of the sampling process in the two domains is then completed by recognizing that convolution of an impulse function with another function simply recreates that function, centered at the impulse function location, and left/right reversed ("reflected"). A train of impulse functions (the comb function) then re-creates replicas of the signal's Fourier transform at each and every impulse function in the train.

This model is illustrated in Figure A-1 for the example case of properly sampling a signal band-limited to 10 cy/mm at 508 ppi (0.050 mm sampling increment), which does not produce aliasing, as compared to undersampling the same signal at 339 ppi (0.075 mm sampling increment), which produces aliasing as low as 3.8 cy/mm. It is these Fourier domain replicas of the signal's transform that impose the limitation of the Nyquist frequency on a sampling system. If other replicas intrude upon the replica centered at zero spatial frequency (the "baseband" replica), then the sampled signal has been corrupted and this corruption is called aliasing, as shown in Figure A-1.

Proper (Nyquist Rate) Sampling



Under Sampling

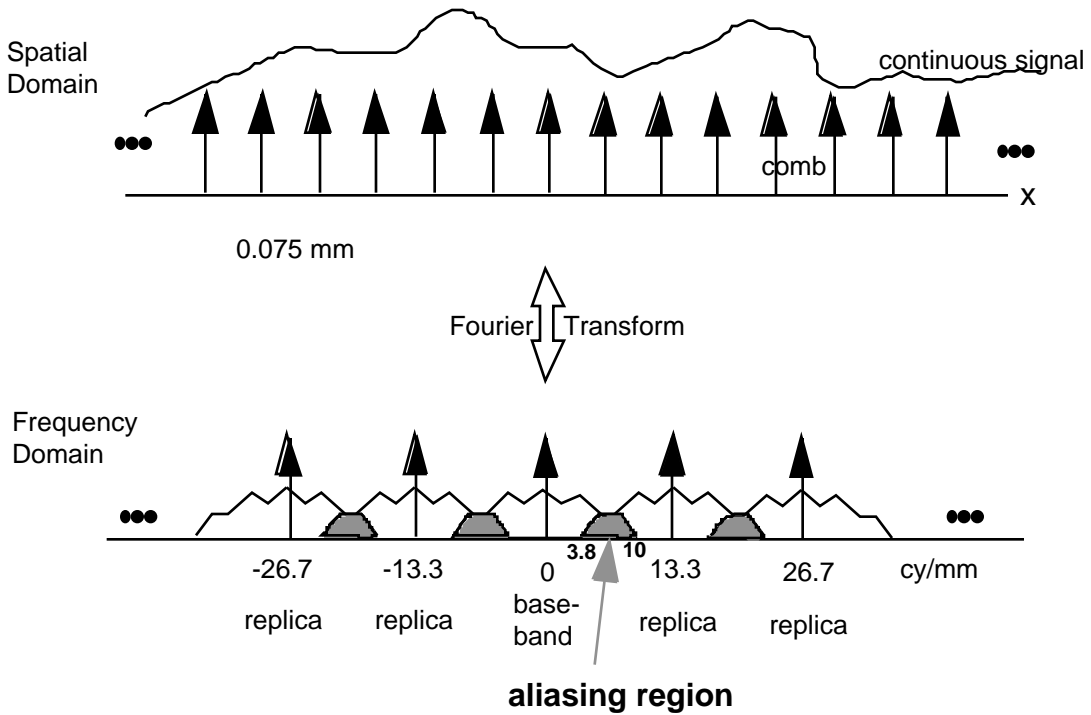


Figure A-1. Proper Nyquist Rate Sampling (Top Half) of a Signal Bandlimited to 10 cy/mm, and Improper Sampling Causing Aliasing (Bottom Half)

APPENDIX B

MODELING DECIMATION

The Fast Fourier Transforms (FFT) of a series of pure digital sinewaves of specified frequencies and sampling resolutions was computed. Decimation was then simulated by dropping every Mth sample prior to the FFT. Since the FFT requires that the number of samples equals a power of 2, the decimated sinewave was generated through multiple periods until the condition was met. A series of FFTs of a variety of decimated sinewaves shows a trend that is consistent with aliasing. Plots of the magnitudes of these FFTs are shown in Figures B-1 through B-4. Each spike in the plots represents a sinewave, whose frequency is given by its location along the frequency axis. Three input sinewaves were used for each of the four plots, which show the results of no decimation, 2:1, 3:2, and 4:3 decimation. It is in comparing this progression of decimations that leads to classifying the artifacts generated by nonuniform decimation as aliasing.

An approach for analyzing aliasing caused by decimation has been given in the literature [Gori and Guattari, 1971]. Although the focus of that work was to devise methods to properly reconstruct nonuniformly sampled signals, it also presented a mathematical model that can be tailored to explain the aliasing resulting from decimation. Nonuniform sampling is modeled as a periodic sampling containing N nonuniformly spaced samples in each period of $N\Delta$, where Δ is the Nyquist sampling period of the signal. An intermediate result of their analysis shows that $2N-1$ replicas of the sampled signal's spectrum appear in the baseband and that these replicas will appear centered around multiples of the frequency $f_0=1/N\Delta$ (refer to Figure A-1 for the meaning of replicas and baseband). The series of plots shown in Figures B-1 through B-4 show exactly this trend. Given that these figures show just the positive half of the spectrum up to the Nyquist frequency of the decimated resolution, each plot should show the original signal spectrum and $N-1$ additional replicas. For example, in 3:2 decimation, $N=2$ and one replica is expected. Each of the four cases agrees with this result. In addition, these replicas are reflected around multiples of the frequency f_0 . In the 3:2 decimation case, f_0 is equal to 7.87 cy/mm, and the negative part of the spectrum appears reflected at the right of the plot. In the 4:3 decimation case, the replication of the entire spectrum is centered around 5.91 cy/mm. These examples support the initial hypothesis that nonuniform decimation causes aliasing of the sampled signal.

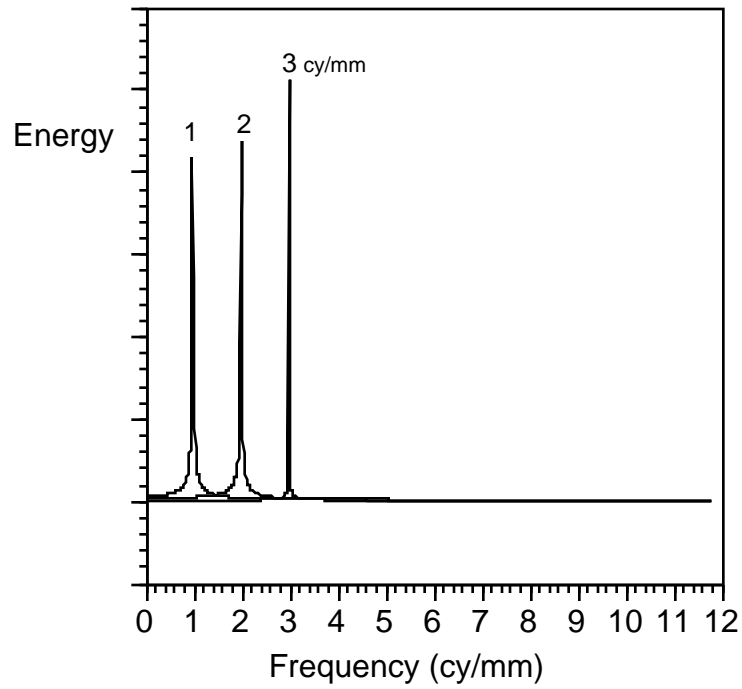


Figure B-1. Spectrum of Three Pure Sinewaves (600 ppi)

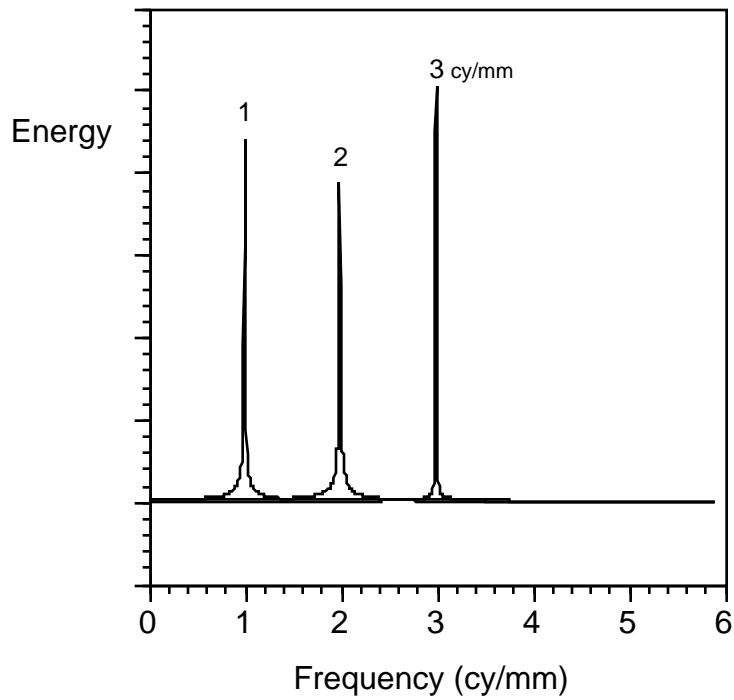


Figure B-2. Spectrum of Three Pure Sinewaves After 2:1 Decimation (300 ppi)

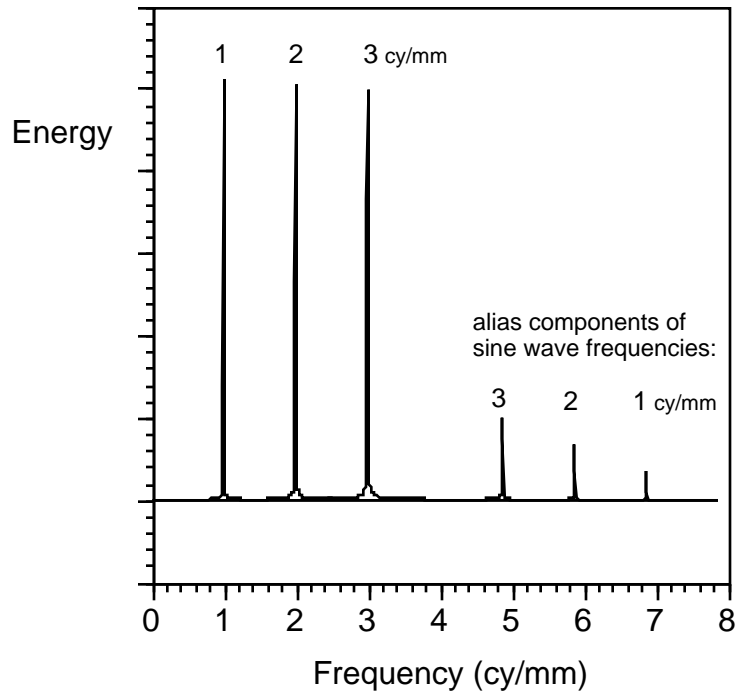


Figure B-3. Spectrum of Three Pure Sinewaves After 3:2 Decimation (400 ppi)

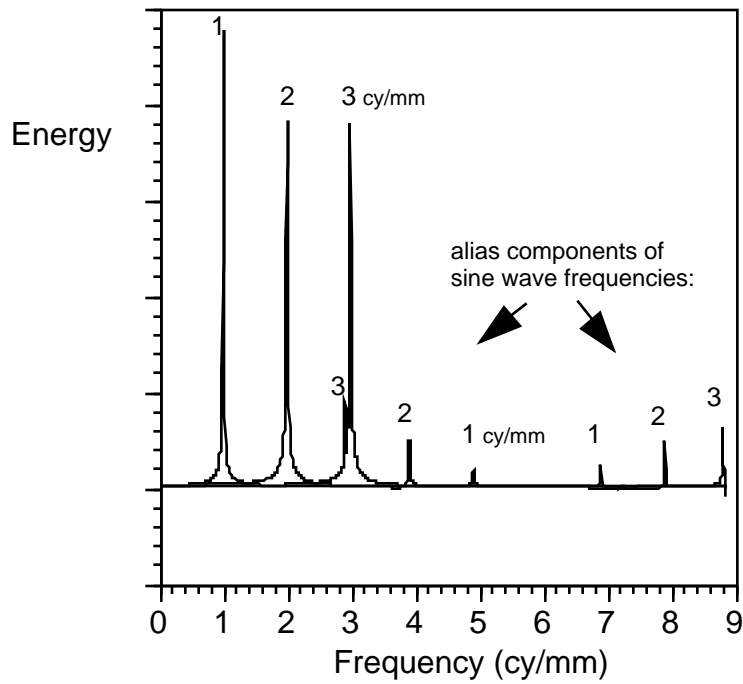
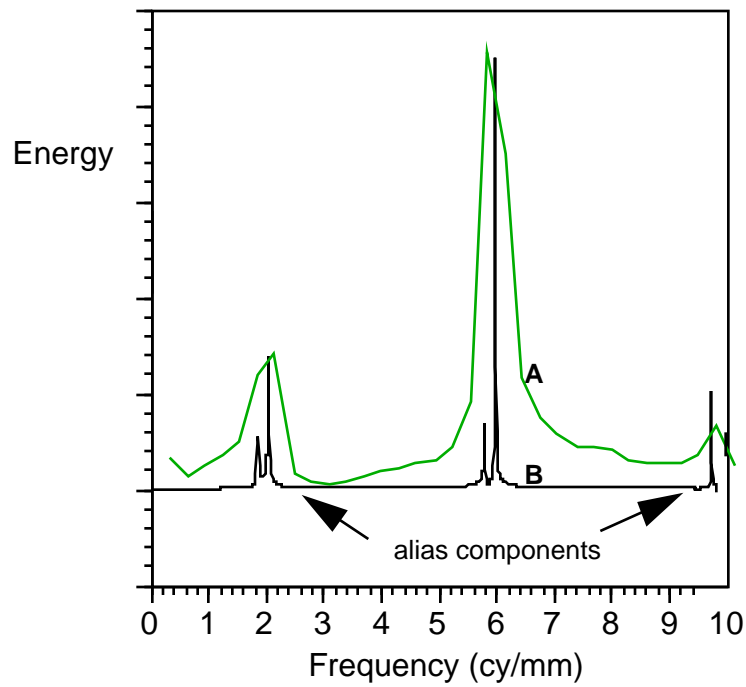


Figure B-4. Spectrum of Three Pure Sinewaves After 4:3 Decimation (450 ppi)

Finally, as an additional check of the analytical modeling procedure, the procedure used in generating Figures B-1 through B-4 was used to model the frequency spectrum of a 6 cy/mm pure sine wave sampled at 600 ppi and decimated to 500 ppi. This was then compared to a real 6 cy/mm sine wave actually scanned at 600 ppi and decimated to 500 ppi (*Eik1* image in Figure 2). As shown in Figure B-5, the analytical model case compares very well with the actual scan case, both show two secondary energy spikes indicative of aliasing caused by the nonuniform 6:5 decimation.



Curve A: |FFT| of actual scanned 6 cy/mm sine wave decimated 6:5
Curve B: |FFT| of analytical model of pure 6 cy/mm sine wave decimated 6:5

Figure B-5. Spectrum of a 6 cy/mm Sinewave After 600 to 500 ppi Decimation

GLOSSARY

AFIS	Automated Fingerprint Identification System
COTS	Commercial Off-The-Shelf
CRT	Cathode Ray Tube
cy/mm	cycles per millimeter
FBI	Federal Bureau of Investigation
FFT	Fast Fourier Transform
IAFIS	Integrated Automated Fingerprint Identification System
IQM	Image Quality Measure
IQS	Image Quality Specification
MTF	Modulation Transfer Function
ppi	pixels per inch
WSQ	Wavelet Scalar Quantization
1-D	One-Dimensional
2-D	Two-Dimensional

